KAZAL-TYPE SERINE PROTEINASE INHIBITORS IN THE MIDGUT OF *PHLEBOTOMUS PAPATASI*

by

LEAH T. SIGLE

B.S., Kansas State University, 2007

A THESIS

Submitted in partial fulfillment of the requirements for the degree

MASTER OF SCIENCE

Department of Entomology
College of Agriculture

KANSAS STATE UNIVERSITY
Manhattan, Kansas

2011

Approved by:

Major Professor
Marcelo Ramalho-Ortigão

Copyright

Abstract

Sand flies (Diptera:Psychodidae) are vectors of parasites of the genus *Leishmania* transmitted to suitable vertebrate host during blood feeding. For blood feeding arthropods, including sand flies, blood meal digestion requires the secretion of inhibitory molecules, such as Kazal-type serine proteinase inhibitors that are involved in preventing the blood from coagulating within the mouthparts and the midgut. Previous studies have identified such molecules in mosquitoes, ticks, and triatomine bugs. Following studies of the midgut transcriptome of *Phlebotomus papatasi*, the principal vector of *Leishmania major*, two non-classical Kazal-type serine proteinase inhibitors were identified (*PpKzl1* and *PpKzl2*). We are interested in the role of these proteins as inhibitors of coagulation cascades, in addition to their potential effects on blood digestion in *P. papatasi*. *Ppkzl1* is similar to thrombin and trypsin inhibitors in triatomines and mosquitoes and *Ppkzl2* is similar to Kazal-type inhibitors in mosquitoes with unknown function. Analyses of expression profiles indicated that although both transcripts are expressed prior to blood feeding in the midgut of *P. papatasi* they are tightly regulated by the blood meal. Reverse genetics studies using RNAi-targeted knockdown of *PpKzl1* and *PpKzl2* by dsRNA injection did not result in a detectable effect on mRNA expression levels. Thus, we expressed a recombinant PpKzl2 in a mammalian expression system (CHO-S free style cells) that was applied to *in vitro* studies to assess activity against various serine proteinases. Recombinant PpKzl2 inhibited chymotrypsin at nanomolar levels and also inhibited thrombin and trypsin at micromolar levels, suggesting that native PpKzl2 is an active serine proteinase inhibitor and may regulate digestive enzymes and thrombin in the midgut. *Leishmania* development within the sand fly midgut is faced with several barriers that can severely impact the parasites. For transmission to occur, parasites must be able to overcome these barriers including digestive proteinases, escape from the peritrophic matrix, and midgut attachment. Early stages of *Leishmania* are susceptible to killing by digestive proteinases in the sand fly midgut. Thus, targeting serine proteinase inhibitors may provide a new strategy to prevent transmission of *Leishmania*.

Table of Contents

List of Figures

List of Tables

Acknowledgements

I would like to thank my major advisor Dr. Marcelo Ramalho-Ortigao for this wonderful opportunity I have had pursuing my Master's in his support at the Department of Entomology, at Kansas State University. His knowledge and enthusiasm for vector biology has been inspiring and encouraging along the way, and I have really enjoyed having him as a mentor. I am also grateful to my committee members Dr. C. Michael Smith and Dr. Kristin Michel for their guidance and critical review of my thesis.

I want to acknowledge all of my colleagues for all the help they have provided and for making the Biology of Disease Vectors laboratory a great place to be. Thanks to Dr. Narinder K. Sharma, Dr. Iliano Coutinho-Abreu and Ms. Maricela Robles-Murguia for all the help they offered in the lab. Thanks to all those helping with sand fly colony maintenance especially Dr. Julin Weng, Dr Kamila Koci, and Ms. Rebekah Allen.

Lastly, the Department of Entomology at Kansas State University has given me this opportunity and I thank the department for providing a great atmosphere in which to study Entomology.

Dedication

I dedicate this thesis to my husband Luke W. Sigle who has always been encouraging and supportive of my endeavors.

Chapter 1 - *Phlebotomus papatasi* Kazal-type Inhibitors

Introduction

Phlebotomine sand flies (Diptera:Psychodidae) are vectors of parasites of the genus *Leishmania*. Transmission of *Leishmania* to suitable vertebrate hosts occurs during blood feeding through the bite site of the sand fly (Ramalho-Ortigão et al. 2010). Leishmaniasis is a neglected disease endemic in 98 countries or territories, putting over 350 million people at risk. Leishmaniasis is a multi-spectrum disease that ranges from cutaneous, diffuse, mucocutaneous to visceral forms, with visceral outcomes leading to an estimated 50,000 deaths annually. While the disease is widely dispersed and transmission to humans occurs on five continents, 90% of the burden of visceral leishmaniasis resides within six countries and 90% of the burden of cutaneous leishmaniasis resides within 10 countries (WHO 2010).

Leishmania sp. are protozoan trypanosome parasites with a digenetic lifecycle. Promastigote forms are found in the alimentary track of sand flies and amastigote forms are found in mammalian macrophages (Bates 2008). Around 40 species of *Leishmania* of medical and veterinary importance have been identified (Ramalho-Ortigão et al. 2010). For vector to host transmission to occur, parasites must develop into the infectious stage within the sand fly. Once a sand fly has ingested an infectious blood meal, *Leishmania* development is restricted to the alimentary track of the sand fly including the midgut and foregut (Kimblin et al. 2008). Parasites are ingested in the amastigote stage along with the blood meal. A chitinous peritrophic matrix (PM) surrounds the blood meal forming a barrier between the ingested blood and the gut epithelial cells. Differentiation into the motile promastigote form occurs within the PM. By 2-3 days post-infection the PM is degraded and parasites escape from the endoperitrophic space where developmental changes in size and shape are observed. Parasites must then attach to the midgut in order to avoid excretion along with the blood meal remnants. Detachment and migration towards the foregut follows with more morphological changes in size and shape. Here at the anterior midgut next to the stomodeal valve is where the infectious metacyclic form differentiates. Complete development to the metacyclic form is around seven days post infection. Finally during the next blood meal metacyclic parasites are regurgitated during feeding and deposited on the wound produced by the tearing action of the sand fly mouthparts (Bates 2007; Ramalho-Ortigão et al. 2010; Sacks 2001).

Over 900 species and sub-species of sand flies have been identified but only about 30-35 are proven or suspected vectors of leishmaniasis (Ramalho-Ortigão et al. 2010). The sand fly and *Leishmania sp.* combination determines the compatibility of parasite development within the vector that can lead to an infectious sand fly. Of the species that are vectors some are restrictive, only infected by a single *Leishmania sp.*, and others are permissive of experimental infections of multiple species (Ramalho-Ortigão et al. 2010). These sand fly-parasite relationships are a balance of vector-parasite interactions leading to either refractory or transmissible infection.

Several barriers to *Leishmania* development within the sand fly including digestive proteinases, escape from the PM, attachment to the midgut to avoid excretion, and migration to the thoracic midgut (Bates 2008; Ramalho-Ortigão et al. 2010; Sacks 2001) must be overcome by the parasites in order to establish a successful infection in the vector. Although not fully understood, it is generally believed that differences in such barriers presented by different sand fly species are related to vector competence in sand flies. Understanding sand fly physiology and parasite-vector interactions at the molecular level is crucial in elucidating why sand flies are such effective vectors.

There is currently no viable vaccine for leishmaniasis. Research geared towards vaccine development continues, and one possible answer to this problem is second-generation vaccines using recombinant proteins to interfere with parasite development (WHO 2010). Transmission blocking vaccines (TBV) are vaccines developed to prevent transmission of the targeted disease. TBVs induce production of antibodies in the host against molecules crucial to parasite development and can be administered to both infected and uninfected individuals to prevent transmission. Such antibodies would interfere with development, hindering parasite differentiation to infectious stages. Target molecules can be insect- or parasite-based proteins. In regards to sand flies and *Leishmania,* TBVs are suggested as a potential way to prevent transmission (Coutinho-Abreu and Ramalho-Ortigão 2010). A TBV for canine visceral leishmaniasis is in use and is affective at interrupting parasite development (Saraiva et al. 2006). This suggests similar strategies could be used in human transmission cycles.

Serine proteinase cascades in arthropods are involved in digestion, coagulation, phenoloxidase activation, and other immune responses. Regulation of these enzymes by serine proteinase inhibitors maintains homeostasis by regulating serine proteinases and their cascades (Di Cera 2009; Jiang and Kanost 2000; Kanost 1999). For blood feeding arthropods, including

sand flies, preventing the blood from coagulating within the mouthparts or the midgut is likely vital for these insects to successfully complete blood feeding and requires the secretion of inhibitory molecules. Previous studies have identified Kazal-type serine proteinase inhibitors that are involved in the inhibition of thrombin and other coagulation cascade factors (Tanaka-Azevedo et al. 2010).

Kazal-type inhibitors are a family of serine proteinase inhibitors that have been characterized in many animals and invertebrates. In blood feeding arthropods thrombin inhibitors have been identified in mosquitoes, ticks, triatomines, and flies (Noeske-Jungblut et al. 1995; Cappello et al. 1998; Francischetti et al. 1999; Campos et al. 2002; Ricci et al. 2007). The first Kazal-type thrombin inhibitor identified in a haematophagous insect was from *Rhodnius prolixus* (Friedrich et al. 1993). Since then, thrombin Kazal inhibitors have been identified in *Triatoma infestans* (Campos et al. 2002), *Triatoma brasiliensis* (Araujo et al. 2007), *Panstrongylus megistus* (Meiser et al. 2010) and *Dipetalogaster maximus* (Mende et al. 1999). These inhibitors found in the gut of these insects inhibit thrombin and blood coagulation cascade factors. Non-Kazal thrombin inhibitors have also been identified in the saliva of *Anopheles albimanus* (Francischetti et al. 1999) and in *Glossina morsitans morsitans* saliva and gut (Cappello et al. 1998). Most recently, a Kazal-type inhibitor from *Aedes aegypti* identified from multiple tissues including salivary glands and the gut was shown to inhibit trypsin and plasmin activity and weakly inhibit thrombin activity (Watanabe et al. 2010).

Inhibition of thrombin by Kazal inhibitors can affect the amount of blood acquired during feeding. Functional characterization, through reverse genetics, of a Kazal-type thrombin inhibitor from *Triatoma brasiliensis* indicated that thrombin inhibition affects blood intake during a blood meal, with the amount of ingested blood decreasing when thrombin inhibition was decreased (Araujo et al. 2007). It has also been shown that blood feeding occurs faster in triatomine species with higher measured anticoagulant activity than other species with lower activity (Paim et al. 2011).

Kazal-type domains are characteristically 40-60 amino acids long and inhibitors may contain single or multiple active domains. Six cysteine residues forming three disulfide bridges distinguish the conserved structure within this family. Outside of the conserved cysteine residues there are high amounts of variability in other amino acid residues (Rimphanitchayakit and Tassanakajon 2010). Tertiary structure of Kazal-type domains includes one α-helix and one anti-

parallel ß-sheet (Schlott et al. 2002). The active site of trypsin-like proteinases binds the substrate and catalyzes the hydrolysis of peptide bonds on the C-terminal side of the P1 residue (Di Cera 2009). Kazal-type inhibitors may or may not be cleaved during inhibition and dissociate at a very slow rate from the enzyme (Kanost and Jiang 1996).

Thrombin is a trypsin-like enzyme that cleaves after arginine and lysine residues. Thrombin has three interaction sites: the active site, the fibrinogen recognition binding site, and a heparin binding site (Tanaka-Azevedo et al. 2010). Multi-domain inhibitors may interact with proteinases at more than one site. An example of this is the two-domain Kazal inhibitor rhodniin, from *R. prolixus*, that interacts with thrombin at the active site and the fibrinogen recognition binding site (van de Locht et al. 1995). Triabin, a single domain inhibitor, binds exclusively to the fibrinogen recognition site, while other inhibitors bind only at the active site (Tanaka-Azevedo et al. 2010).

In the midgut transcriptome of *Phlebotomus papatasi*, the principal vector of *Leishmania major*, two Kazal-type serine proteinase inhibitors were identified, *PpKzl1* and *PpKzl2* (Ramalho-Ortigão et al. 2007). These were the first Kazal-type serine proteinase inhibitors identified from sand flies. The putative PpKzl1 and PpKzl2 are predicted to be secreted in the midgut due to the presence of signal peptides. PpKzl1 and PpKzl2 have only 24% identity and 35% similarity in amino acid sequences. PpKzl1 is similar to Kazal-type inhibitors with anti-hemostatic effects from triatomine species and is also similar to Kazal-type inhibitors from mosquitoes. Both PpKzl1 and PpKzl2 show similarity to putative proteins from the *Lutzomyia longipalpis* EST database (Ramalho-Ortigão et al. 2007).

We hypothesize that two transcripts previously identified in *P. papatasi* as coding for Kazal-type inhibitors are in fact responsible for the expression of two distinct proteins. Moreover, we believe the two Kazal-type inhibitors are secreted into the midgut of *P. papatasi* where one or both assist in maintaining blood fluidity during blood meal digestion. We are interested in the role of these proteins in *P. papatas*i as inhibitors of thrombin. In addition to their potential effects on blood digestion, we aim to assess the potential use of these sand fly midgut proteins as TBV candidates.

The objectives of this study are:

1. Analyze the sequences of the putative PpKzl1 and PpKzl2 for predicted activity and similarity.

2. Evaluate the expression of *PpKzl1* and *PpKzl2* in the midgut before and after a blood meal.
3. Assess silencing effects of knockdown of *PpKzl1* and *PpKzl2* during blood meal digestion.
4. Conduct *in vitro* analysis of inhibition activity of a recombinant PpKzl2 protein.

Materials and Methods

Use of animals was preapproved by the Kansas State University Institutional Animal Care and Use Committee (IACUC) under protocols 2747, 2748 and 2749.

Sand fly rearing and dissections

P. papatasi Israel (PPIS) and *P. papatasi* Jordan (PPJO) strains were reared in the Biology of Disease Vectors laboratory at the Department of Entomology, Kansas State University. Flies were maintained on 30% sucrose solution at 27 ºC and 70% humidity. For blood feeding, sand flies were allowed to feed for approximately 30 min on a BALB/c mouse anesthetized with 3 mg ketamine (Ketaset, Fort Dodge Animal Health, Fort Dodge, IA), and 0.12 mg xylazine (AnaSed, Acorn Inc, Decatur, IL) per mouse (100 mg/kg of ketamine; and 3 mg/kg of xylazine). At 20 h post-blood meal all blood-fed flies were briefly anesthetized with CO_2 and examined under a dissecting microscope. Fully fed flies (i.e., abdomen fully distended) of similar size were selected for dissection. Midguts were dissected in 30 µl 1x PBS buffer RNAse free (Fisher) with ELIMINase (Fisher, Scientific, Pittsburgh, PA,) treated tools and equipment. Dissected midguts were then transferred to 50 µl of RNA later (Qiagen, Valencia, CA), homogenized with a hand-held homogenizer for approximately 20 sec and placed at -80 ºC.

Sequence analysis

PpKzl1 and *PpKzl2* were previously indentified from *P. papatasi* cDNA midgut libraries (Ramalho-Ortigão et al. 2007). Molecular weights and isoelectric points (pI) were predicted using the Swiss Institute of Bioinformatics ExPASy tools (Gasteiger et al. 2003). Sequences similar to PpKzl1 and PpKzl2 were indentified in NCBI using BLASTP for the non-redundant protein database (Altschul et al. 1997). Sequences were selected from matches with E value $\leq 10^{-5}$ for use in multiple sequence alignments. The region including the six conserved cysteine residues in PpKzl1 and PpKzl2 was used for multiple sequence alignment. Protein sequence alignments were performed using ClustalW2 (Larkin et al. 2007) and manual edits were performed in Jalview Version 2 (Waterhouse et al. 2009).

PpKzl2 was blasted in the *L. longipalpis* Llon 0.1 preliminary Genome assembly on the Baylor College of Medicine Human Genome Sequencing Center website. A sequence was

identified and translated with Swiss Institute of Bioinformatics ExPASy and referred to *as L. longipalpis* Kzl2 (Gasteiger et al. 2003; Ramalho-Ortigão et al. 2003).

RNA extraction and cDNA synthesis

Total RNA was extracted from midgut samples using the RNeasy Mini Kit (Qiagen, Valencia, CA) and eluted in 40 µl of RNase-free water. Extracted RNA was treated with TURBO DNase (Ambion, Austin, TX) to eliminate any residual genomic DNA. Up to 100 ng of each RNA was used for first strand cDNA synthesis and was added to 3.3 µM Oligo-dT_{20} primer, 0.67 mM dNTPs and RNase-free water to total volume of 15 µl. Samples were incubated at 65 ºC for 5 min and then placed on ice for 1 min. Addition of 4 µl of 5x SuperScript III Reverse Transcriptase First-Strand Buffer, 5 mM DTT, 0.5 µl RNaseOUT (40 units/µl) and 1 µl of SuperScript III Reverse Transcriptase (200 units/µl) was followed with 1 h incubation at 50 ºC. All reagents for cDNA synthesis were purchased form Invitrogen (Carlsbad, CA) and cDNA was stored at -20 ºC.

Real-time PCR

PpKzl1 and *PpKzl2* relative expression was analyzed in non blood-fed and blood-fed adult female sand flies. Individual midguts were dissected from non blood-fed flies (0 h) and blood-fed flies at 24, 48 and 72 h post-blood meal. Total RNA was extracted from individual midguts and used for first-strand cDNA synthesis. Real-Time PCR (rt-PCR) was carried out on an Eppendorf Mastercycler ep Realplex^4 in 8 µl reactions. Forward and reverse 0.3 µM primers (Table 1) were mixed with 4 µl iQ SYBR green Supermix (BioRad, Hercules, CA) and added to 0.2 µl cDNA and 3.32 µl molecular grade water (Invitrogen, Carlsbad, CA). All cDNA samples were run in duplicate for *PpKzl1* and *PpKzl2* and in parallel for *40S ribosomal protein S3* (GenBank accession number: FG113203). Reactions were carried out: 40 cycles of 95 ºC/30 sec, of 58 ºC/1 min, and 72 ºC/30 sec, followed by 95 ºC/15 sec, 60 ºC/15 sec, and a melt curve up to 95 ºC /20 min. C_T values from the Realplex Software were used for expression analysis.

Expression levels of mRNA were calculated with the delta-delta C_T method. C_T values were normalized to the expression of a non-regulated internal control gene, *40S ribosomal protein S3,* and then normalized to a calibrator for temporal analysis. Temporal analysis: $\Delta\Delta C_T = [(C_T \text{ PpKzl1} - C_T \text{ 40s-S3})_{\text{Time X Sample 1}}] - [\text{Average}_{\text{All Time 0 Samples}} \{(C_T \text{ PpKzl1} - C_T \text{ 40s-S3})_{\text{Time 0 Sample 1}}\}]$. Fold change was calculated by $2^{-\Delta\Delta CT}$ (Livak and Schmittgen 2001). Logarithmic

transformation of data gave a normal distribution as confirmed by the Kolmogorov-Smirnov test for normality and Levene's test for equality of variance. Transformed data was evaluated with one-way analysis of variance (ANOVA) and a parametric t test with the Bonferroni correction for multiple comparisons. Expression differences in the means of individual midguts between time points 0, 24, 48 and 72 h post-blood meal were determined at p-values: $p < 0.05$, $p < 0.01$, and $p < 0.001$. Prism 5 Software (GraphPad, La Jolla, CA) was used for all graphing and statistical analysis.

For analysis of dsRNA injected sand flies, relative expression levels of mRNA were quantified with the comparative C_T method. C_T values were normalized to the expression of *40S ribosomal protein S3*, $\Delta C_T = (C_T \text{ Target gene }_{\text{Sample 1}}) - (C_T \text{ 40s-S3 }_{\text{Sample 1}})$, and then transformed to $2^{-\Delta CT}$ (Schmittgen and Livak 2008). Relative expression of the target gene in dsPpKzl1 or dsPpKzl2 injected flies were compared to expression in the control dsGFP injected flies at similar time points post-injection and post-blood meal. Prism 5 Software (GraphPad, La Jolla, CA) was used for all graphing and statistical analysis. A two-tailed Mann-Whitney U test was used for nonparametric statistical comparison of expression in dsPpKzl2 and dsGFP injected flies. Data was first checked for normality using the Kolmogorov-Smirnov test.

dsRNA synthesis

PCR of DNA templates used in dsRNA synthesis were amplified using touchdown PCR to obtain clean templates with primers PpKzl1_T7i and PpKzl2_T7i (Table 1). Both forward and reverse primers contained a full length T7 promoter at the 5' end. Green fluorescence protein PCR product with flanking T7 promoters was amplified with a T7 primer. For these reactions 5 µl of 5x GoTaq buffer, 1.5 mM $MgCl_2$, 0.2 mM dNTPs, 0.2 µM forward and reverse primers, 1 µl cDNA template, 1.25 units GoTaq DNA Polymerase and molecular grade water to 25 µl total were combined and mixed. All reagents were purchased from Promega, Madison, WI. Touchdown PCR was as follows, 5 cycles of 95 ºC/3 min, 94 ºC/1 min, 72 ºC/1 min, 5 cycles of 94 ºC/1 min, 68 ºC/1 min, 72 ºC/1 min, 30 cycles of 94 ºC/1 min, 55 ºC 1 min, 72 ºC 1 min, finished with 72 ºC 5 min.

DNA templates were purified and concentrated on YM-100 filters (Millipore, Billerica, MA), checked on 1.5% agarose ethidium bromide gel and quantified with Biotek Epoch Gen5 Take3 Module (Biotek, Winooski, VT). Double-stranded RNA was synthesized with the

TranscriptAid T7 High Yield Transcription Kit (Fermentas, Glen Burnie, Maryland). Briefly, reagents were combined at room temperature in the following order: diethylpyrocarbonate (DEPC)-treated water (to total 20 µl), 4 µl 5x TranscriptAid Reaction Buffer, 40 mM ATP/CTP/GTP/UTP mix, 1 µg Template DNA, and 2 µl TranscriptAid Enzyme Mix. Reactions were carried out at 37 ºC for 2 h and followed with a nuclease digestion with 2 units of DNase1, RNase-free at 37 ºC for 15 min for DNA template removal. Addition of 2 µl of 0.5 M EDTA, pH 8.0 was followed with incubation at 65 ºC for 10 min. Transcripts were purified with phenol:chloroform extraction and ethanol precipitation and resuspended in 20 µl DEPC-treated water. Samples were stored at -20 ºC. Purified dsRNA was checked on a 1.5% agarose ethidium bromide gel and quantified with Biotek Epoch Gen5 Take3 Module (Biotek, Winooski, VT). Final concentrations for injection were 4.0-5.5 µg/µl.

dsRNA injection

Flies 3-5 days old were anesthetized briefly with CO_2 and maintained on ice for dsRNA microinjection. Flies were injected in the thorax using a Nanoject II (Drummond Scientific, Broomall, PA) with 23 nl of dsRNA for either the target gene (*PpKzl1* or *PpKzl2*) or control green fluorescence protein gene (dsGFP) (Arakane et al. 2008). After injections flies were maintained at 85% humidity until dissection or blood feeding. Flies were allowed to feed on an anesthetized naïve BALB/c mouse 48 h post-injection. After the blood meal flies were maintained on 30% sucrose solution. Midguts were dissected at specific time points post-blood meal for RNA extraction, cDNA synthesis and rt-PCR as described above.

Hemoglobin assay

The rate of digestion of dsRNA injected sand flies was assessed post-blood meal with a hemoglobin assay. Hemoglobin was measured with a colorimetric assay using Drabkin's solution. Drabkin's solution was prepared by adding 5 µl of Brij 35 30% solution to 10 ml of Drabkin's Reagent and mixing well (Sigma, Saint Louis, MO). Flies were injected as described above and fed on an anesthetized naïve BALB/c mouse 48 h post-injection. Midguts were dissected 24 and 48 h post-blood meal as described above with exception that midguts were homogenized in 250 µl of Drabkin's solution. Samples were transferred to a 96-well microtiter plate and incubated for 15 min at room temperature (23 ºC). Absorbance at 540 nm was recorded on a Biotek Epoch Gen5 (Biotek, Winooski, VT). Know quantities of mouse blood were

measured as a standard. The mean of individual midguts at each time point were analyzed with a two-tailed unpaired t test. Normality was tested with the Kolmogorov-Smirnov test. Pictures of dissected midguts were taken using an AM423X Dino-Eye camera (Dinolite, Songshan District, Taipei, Taiwan).

Recombinant protein expression and purification

The mature (minus signal peptide) *PpKzl2* cDNA was amplified using the forward primer PpKzl859 and the reverse primer PpKzl2-R-His containing a 6x-His tag on its 3' end (C-terminus) (Table 1), touchdown PCR was performed using conditions as listed above. Two microliters of the PCR product was separated on an agarose gel for analysis and to assess concentration. One microliter of PCR product (corresponding to 20 ng) was used to ligate into the VR1020-TOPO vector (Oliveira et al. 2006). Four microliters of the ligation reaction was used to transform *E. coli* Top10 competent cells (Invitrogen, Carlsbad, CA) for a 30 minute incubation on ice, followed by a heat shock at 42 ºC for 50 sec, ice for 2 min, addition of 500 µl LB media and incubation shaking at 37 ºC for 60 min. Transformed cells were plated on LB plates supplemented with 50 µg/ml Kanamycin and incubated at 37 ºC overnight. Colonies were screened by PCR with VR1020 primers (Table 1) and orientation was confirmed by sequencing. The Endofree Plasmid Mega Kit (Qiagen, Valencia, CA) was used for plasmid purification following the manufacturer's protocol and was followed by four washes with 12-15 ml of nuclease-free water using an Amicon-Ultra filter with a cutoff value of 100 kDa (Milipore, Billerica, MA). Final concentration was 2.5 mg/ml. The plasmid sequence was confirmed by DNA sequencing in both directions with forward and reverse VR1020 primers. DNA sequencing was performed at the DNA Sequencing and Genotyping Facility, Kansas State University.

Recombinant protein was expressed in CHO-S free style cells. Transfection into the CHO-S free style cells began with separate dilutions of 37.5 µg of purified plasmid DNA and 37.5 µl of FreeStyle MAX reagent in 0.6 ml OptiPro serum free media. Both dilutions were mixed together by inversion in a 1.5 ml tube and incubated at room temperature for 10 min. Then the DNA-MAX reagent mixture was dispensed in small aliquots to $1x10^6$ CHO-S free style cells in 30 ml expression medium in a 125 ml round bottom flask (BD Biosciences, Sparks, MD). Transfected cells were incubated at 37 ºC with an atmosphere of 8% CO_2 with shaking at 125

rpm. At 72 h culture supernatant was collected and concentrated using Centricon filters (Milipore, Billerica, MA) with a cutoff value of 3 kDa.

Recombinant PpKzl2 (rPpKzl2) was purified by nickel-nitrilotriacetic acid (Ni-NTA) chromatography with a gravity flow column. Briefly, the concentrated protein obtained from CHO-S cells was washed using Centricon filters (Millipore) with a cutoff value of 3 kDa with PBS five times, and loaded onto 1 ml Ni-NTA in a 5 ml syringe (BD Biosciences). Washes on the column included 15 ml of wash buffer (20 mM Sodium phosphate buffer, 300 mM sodium chloride, and 20 mM Imidazole), and final elution with 5 ml of elution buffer (20 mM Sodium phosphate buffer, 300 mM sodium chloride, and 300 mM imidazole). The eluted rPpKzl2 was concentrated to 1.5 µg/µl. Two hundred and fifty nanograms of protein were analyzed by SDS-PAGE using 4-12% reducing Bis-Tris NuPAGE pre-cast gel purchased from Invitrogen (Carlsbad, CA). The protein was transferred to nitrocellulose and incubated with anti-His antibody (Santa Cruz, Santa Cruz, CA) overnight at 4ºC and followed by three washes of 10 minutes each in TBS-T (TBS buffer with 0.1% tween-20). The blot was incubated with anti-mouse antibody conjugated to alkaline phosphatase (Promega, Madison, WI) diluted 1:10,000 in TBS-T for 1 hour at room temperature and washed in TBS-T. The protein bands were visualized using the Western Blue substrate (Promega, Madison, WI) (Figure 10).

Inhibition assays

The inhibition activity of rPpKzl2 was tested against human α-thrombin and trypsin, and bovine α-chymotrypsin . Increasing concentrations of rPpKzl2 were pre-incubated with 0.05 µM human α-thrombin (Calbiochem, EMD Chemicals Inc., Gibbstown, NJ), 2 µM trypsin (Sigma, St. Louis, MO), or 0.25 µM α-chymotrypsin (Calbiochem, EMD Chemicals Inc., Gibbstown, NJ) in 50 mM Hepes-0.5% BSA, pH 7.3 for thrombin, and in 50 mM Tris-HCl, pH 8.0 for trypsin and α-chymotrypsin. The enzyme and rPpKzl2 incubated for 15 min at 37 ºC in a 96-well non-binding microtiter plate. Chromogenic peptide substrate H-D-Phenylalanyl-L-pipecolyl-Larginine-p-nitroaniline dihydrochloride (S-2238) (Chromogenix, diaPharma, West Chester Township, OH), Na-Benzoyl-D,L-arginine 4-nitroanilide hydrochloride (BAPNA) (Sigma, St. Louis, MO), or N-Succinyl-L-alanyl-L-alanyl-L-prolyl-L-phenylalanine 4-nitroanilide (Suc-AAPF-pNA) (Sigma, St. Louis, MO) was added at increasing concentrations for thrombin, trypsin, or α-chymotrypsin respectively for a total reaction volume of 100 µl. Trypsin activity

was measured for 3 nM, 30 nM, and 300 nM rPpKzl2 at increasing concentrations of BAPNA (25 µM, 125 µM, 250 µM, 500 µM, and 1000 µM). Inhibition of α-chymotrypsin activity was measured with 0.0005 nM, 0.005 nM, and 0.05 nM rPpKzl2 at increasing concentrations of Suc-AAPF-pNA (250 µM, 500 µM, and 1000 µM). Inhibition of thrombin activity was measured at 0.5 nM, 3 nM, and 300 nM rPpKzl2 at 500 µM and 1000 µM S2238. The rate of proteinase hydrolysis of the chromogenic substrate was measured at 405 nm with a Biotek Synergy HT microplate reader (Biotek, Winooski, VT).

Graphs of initial velocity (V) versus substrate concentration were fit with the Michaelis-Menten Equation to obtain the kinetic constant (K_m) and Maximum Velocity (V_{max}), $v = \frac{V\max[S]}{Km + [S]}$ (Copeland 2000). Obtained V_{max} values from reactions with rPpKzl2 were then compared to the V_{max} of 0 nM rPpKzl2 to calculate residual activity, residual activity = $\frac{V\max}{V\max,0}$ (Copeland 2005). The dissociation constant αK_i was calculated with the Michaelis-Menten Equation for uncompetitive inhibition, $v = \frac{\frac{V\max[S]}{1+[I]/\alpha Ki}}{\frac{Km}{1+[I]/\alpha Ki} + [S]}$ (Copeland 2000).

Results

Sequence analysis

Both *PpKzl1* and *PpKzl2* code for non-classical Kazal-type inhibitors. Non-classical Kazal-type inhibitors are distinguished from classical Kazal-type by differences in positions of the six conserved cysteine residues (Augustin et al. 2009; Hemmi et al. 2005). Both classical and non-classical Kazal-type inhibitors have six cysteines forming three disulfide bridges between C_1:C_5, C_2:C_4, C_3:C_6. In non-classical Kazal-type inhibitors the disulfide bridge formed by C_1 and C_5 is shifted closer to the C-terminus (Hemmi et al. 2005). The predicted reactive site P1 amino acid residue is located at position C_2-X-P1 and determines specificity within Kazal-type inhibitors.

The *PpKzl1* cDNA sequence is 620 bp and encodes a 78 amino acid protein containing a single Kazal-type domain (GenBank accession number: EU045342), and estimated molecular weight of 6.4 kDa and 5.22 pI. *PpKzl1* encodes a predicted signal peptide including a cysteine residue (separate from the six cysteines in the Kazal domain) and is cleaved at residues 21-22 suggesting that the mature PpKzl1 is secreted in the midgut. PpKzl1 possesses six predicted conserved cysteine residues distinguishing it as a non-classical Kazal-type domain. It also has other conserved patterns found in other non-classical Kazals; a conserved region P-X-C_3-G, and a conserved T-Y between C_3 and C_4 (Augustin et al. 2009). The predicted residue at P1 in PpKzl1 is arginine (Figure 1).

The *PpKzl2* 764 bp cDNA sequence encodes an 89 amino acid protein with predicted molecular weight of 7.6 kDa and 6.10 pI (GenBank accession number: ES349048). A predicted signal peptide cleaved at residues 19-20 suggests that the mature PpKzl2 is secreted in the midgut as well. The mature PpKzl2 also has 6 predicted conserved cysteine residues, but location of the fourth and fifth cysteine residues differ from PpKzl1. However, it is still characteristic of a non-classical Kazal-type domain (Figure 1). The predicted residue at P1 in PpKzl2 is tyrosine.

Arginine in the P1 site has been shown to confer thrombin and trypsin inhibitory activities (Kanost 1999). It has also been shown to inhibit other trypsin-like serine proteinases such as plasmin, factor XIIa, and factor Xa (Campos et al. 2004). Tyrosine in the P1 specifies

chymotrypsin inhibitory activity and also has been shown to inhibit other chymotrypsin-like proteinases such as proteinase K, and cathepsin G (Kanost 1999).

The putative PpKzl1 is similar to other insect Kazal-type inhibitors. An alignment of PpKzl1 with other Kazal-type inhibitors from both blood-feeding and non blood-feeding insects shows a high conservation of cysteine residues and other residues within the six cysteine region for this group of non-classical Kazal-type inhibitors (Figure 2). These inhibitors all have arginine in the P1 active site. With such similarities in overall domain sequence and active residues, functional similarities are proposed. A Kazal inhibitor from *Aedes aegypti* (AaTi) with similarities to PpKzl1 inhibits trypsin and plasmin and weakly inhibits thrombin activity (Watanabe et al. 2010). PpKzl1 is similar to the multi-domain Kazal inhibitor infestin from *T. infestans.* While the multi-domain infestin inhibits thrombin, PpKzl1 is most similar to infestin domain-4 which strongly inhibits Factor XIIa, as well as plasmin and trypsin and does not inhibit thrombin (Campos et al. 2002; Campos et al. 2004). Dipetalogastin is a multi-domain thrombin inhibitor from *D. maximus*. PpKzl1 is most similar to domain 6, part of a post-translational active 2 domain (5-6) peptide, which inhibits thrombin, trypsin, and plasmin and not chymotrypsin or Factor Xa (Mende et al. 2004). A putative protein identified in the New World sand fly *L. longipalpis,* also a vector of *Leishmania sp.,* is most similar to PpKzl1, with 73% identity and 81% similarity (Pitaluga et al. 2009). Other Kazal domains without functional annotation in the alignment include an *Anopheles darlingi* protein (1 of 3) having a Kazal domain (Calvo et al. 2009), a *Culicoides sonorensis* protein (Campbell et al. 2005), and an *Ochlerotatus triseriatus* salivary protein.

The putative PpKzl2 had less similarity with other proteins than PpKzl1. An alignment of PpKzl2 with similar protein sequences shows more divergence in the P1 site and surrounding residues (Figure 3). PpKzl2 is most similar to a putative protein in *L. longipalpis* having 44% identity and 53% similarity. The *L. longipalpis* sequence has a phenylalanine in the predicted P1 site. PpKzl2 is similar to Kazal-type domains from multiple dipteran species and also lepidopteran and hymenoptera species. There has been less functional characterization of this group of Kazal inhibitors. The *Lonomia obliqua* Kazal-type inhibitor was identified in a cDNA library from bristles, venomous structures of the caterpillar, known to cause hemorrhagic symptoms in humans (Veiga et al. 2005). The silkmoth, *Antheraea mylitta,* Kazal-type inhibitor was identified from bacteria-challenged larval fat body EST libraries (Gandhe et al. 2006). A

putative Kazal-type inhibitor similar to PpKzl2 was identified from immuno-activated cDNA libraries from *Ae. aegypti*. The mRNA from hemocytes of bacteria-inoculated (*Escherichia coli* and *Micrococcus luteus*) *Ae. aegypti* larva contained a putative Kazal-type domain (Bartholomay et al. 2004).

PpKzl1 and *PpKzl2* though both non-classical Kazal-type inhibitors have different compositions of the six cysteine domain. They display 24% identity and 35% similarity in amino acid sequences. *PpKzl1* is similar to thrombin and trypsin inhibitors in triatomines and mosquitoes, and *PpKzl2* is similar to a different set of inhibitors within mosquitoes, as well as moths, bees and wasps.

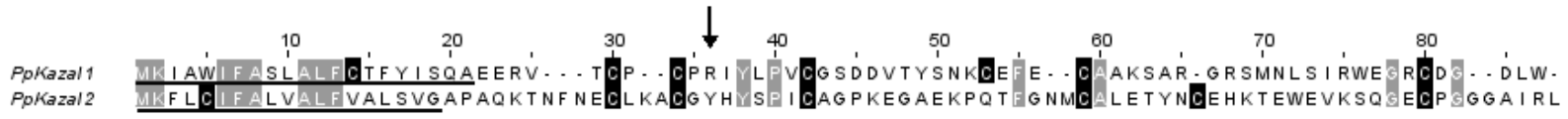

Figure 1 PpKzl1 and PpKzl2 predicted amino acid sequence alignment. PpKzl1 **(**GenBank: EU045342**)** and PpKzl2 **(**GenBank: ES349048) predicted amino acid sequence. Arrow indicates the P1 residue, cysteine residues are in black, all other conserved residues are in gray, gaps are indicated by dashes, and signal peptide sequences are underlined.

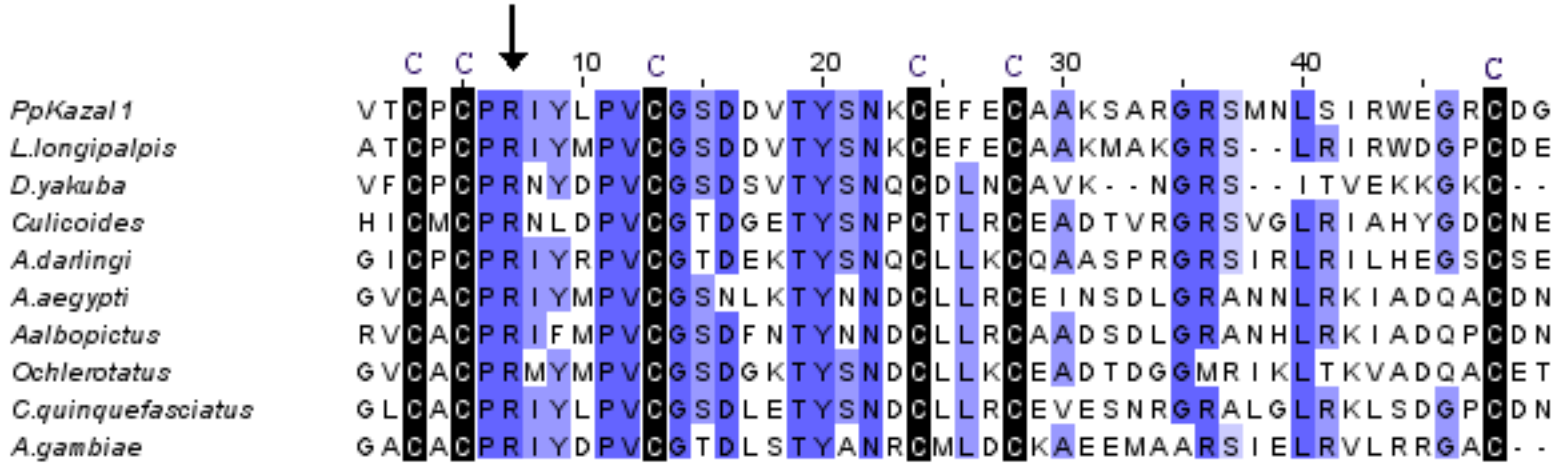

Figure 2 PpKzl1 multiple sequence alignment. *P. papatasi* PpKzl1 **(**EU045342**)** *C. sonorensis* (AAV84258), *Drosophila yakuba* (XP_002088400), *An. darlingi* (ACI30143), *L. longipalpis* (ABV60319), *Ae. aegypti* AaTi (ABF18209), *Culex quinquefasciatus* (XP_001868221), *O. triseriatus* salivary (ACU30983), *Aedes albopictus* (AAV90671), and *Anopheles gambiae* (AGAP007906). Arrow indicates the predicted P1 residue, gaps are indicated by dashes, conserved cysteines (C) are in black, and residues with more than 60% conserved identity are in blue.

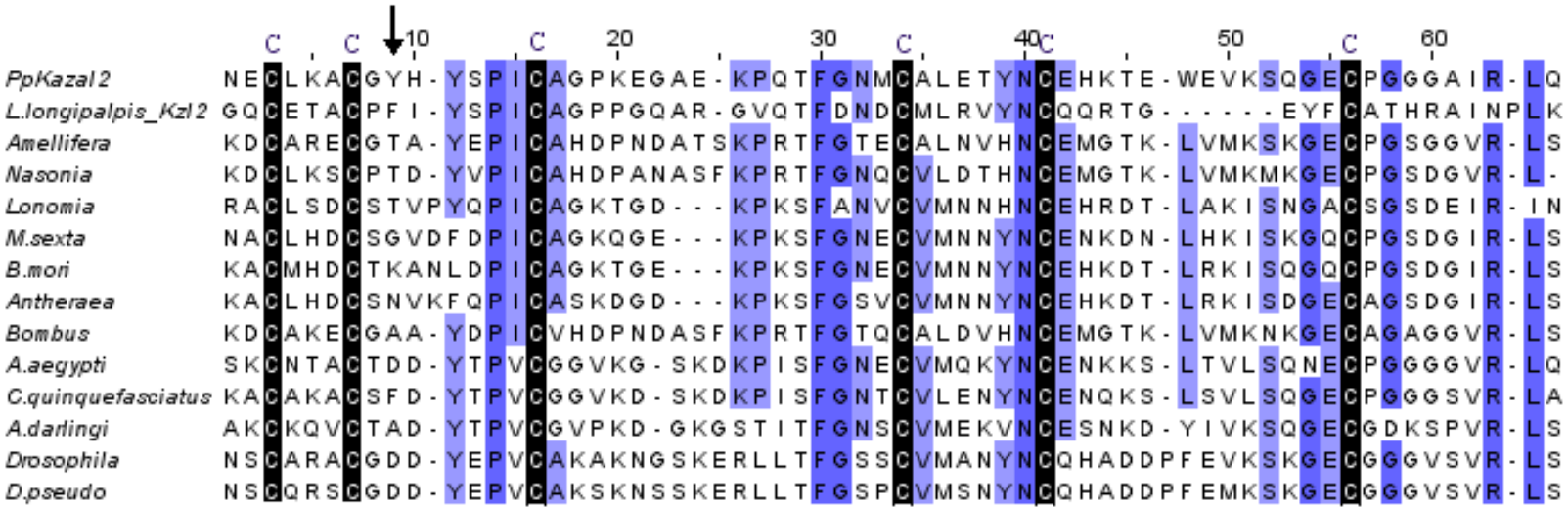

Figure 3 PpKzl2 multiple sequence alignment. *An. darlingi* (ACI30165), *Drosophila mojavensis* (XP_002000106), *Cx. quinquefasciatus* (XP_001842298), *Ae. aegypti* (XP_001658905), *Manduca sexta* (AF117576), *Nasonia vitripennis* (XP_001600330), *Bombyx mori*, (NP_001040250), *Bombus terrestris* (XP_003401213), *Drosophila pseudoobscura pseudoobscura* (GA21026), *A. mylitta* (ABG72727), *L. obliqua* (AAV91449), *Apis mellifera* (XP_392053), and *L. longipalpis* (contig 69115) Arrow indicates the predicted P1 residue, gaps are indicated by dashes, conserved cysteines (C) are in black, and residues with more than 60% conserved identity are in blue.

Expression profiles

Relative expression of *PpKzl1* and *PpKzl2* mRNA transcripts in the midgut were analyzed using rt-PCR and the delta-delta C_T method. Temporal expression levels for 24, 48, and 72 h post-blood meal were calculated as fold change calibrated to 0 h expression. Both *PpKzl1* and *PpKzl2* are expressed constitutively in the midgut. Expression levels of both transcripts are also regulated by blood feeding. *PpKzl1* transcript expression was up-regulated at 24 and 48 h post-blood meal with p-values less than 0.05 and 0.001 respectively. After up-regulation significantly increasing at 48 h post-blood meal, expression of *PpKzl1* between 48 and 72 h was down-regulated reaching a level similar to 0 h expression ($p < 0.01$) (Figure 4 A). Expression of *PpKzl2* was up-regulated 24, 48, and 72 h post-blood meal. Transcript levels were up-regulated at 24 h ($p < 0.01$) and continue to increase significantly at 48 h post-blood meal ($p < 0.001$). A down-regulation occured between 48 and 72 h ($p < 0.001$) with expression levels at 72 h similar to expression at 24 h post-blood meal. While expression decreased at 72 h post-blood meal there was still up-regulation in comparison to 0h expression (Figure 4 B).

Relative expression analysis of *PpKzl1* and *PpKzl2* mRNA showed similarities in expression profiles. *PpKzl1* and *PpKzl2* were both constitutively expressed and up-regulated at 24 and 48 h post-blood meal with a decrease in expression between 48 h and 72 h. Fold change of *PpKzl1* and *PpKzl2* were compared at each time point. The mean fold change at 0, 24, and 72 h post-blood meal were similar for *PpKzl1* and *PpKzl2*. However at 48 h post-blood meal *PpKzl2* was significantly higher than *PpKzl1*. The fold change of *PpKzl2* was significantly different from *PpKzl1* ($p < 0.05$) (Figure 4C). Differences between the means of individual midguts at each time point were determined with a parametric t test and the Bonferroni correction.

A.

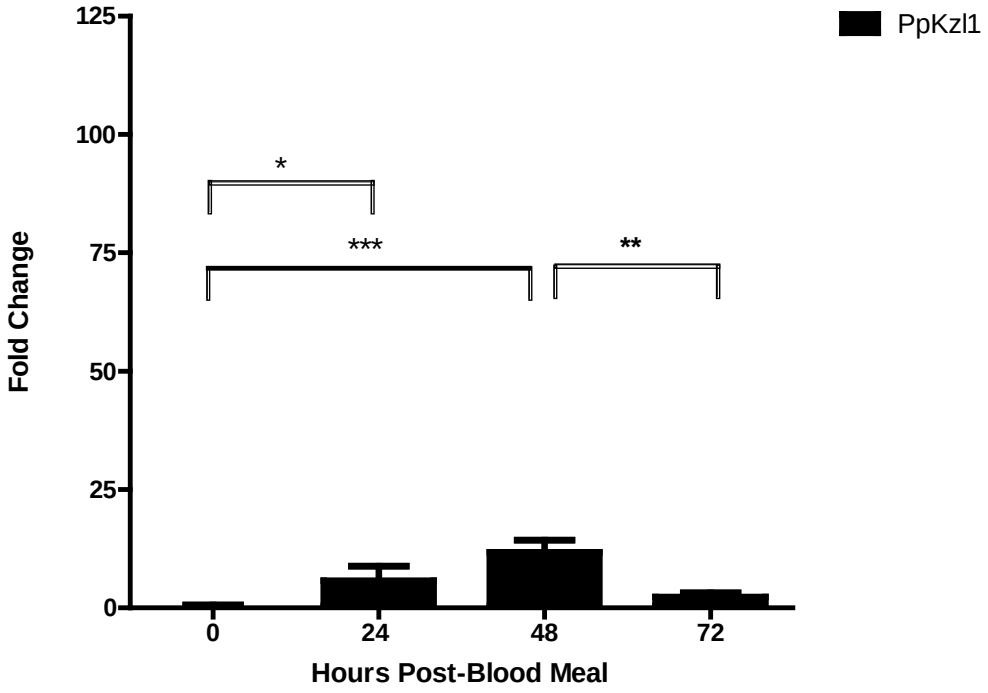
PpKzl1
125
100
75
50
25
0
Fold Change
*
***
**
0
24
48
72
Hours Post-Blood Meal

B.

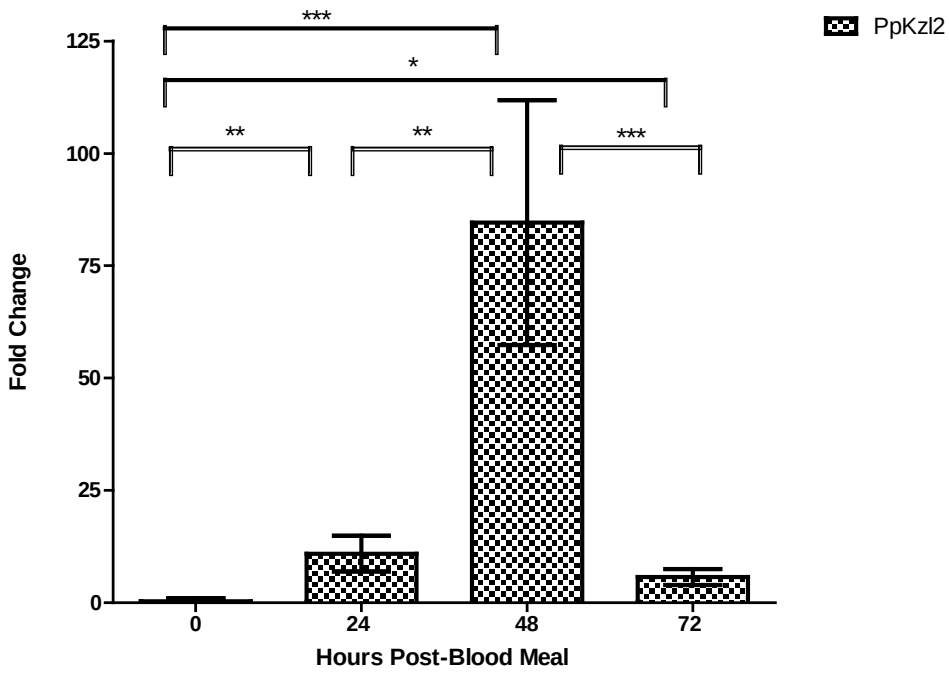
PpKzl2
***
*
**
**
***
125
100
75
50
25
0
Fold Change
0
24
48
72
Hours Post-Blood Meal

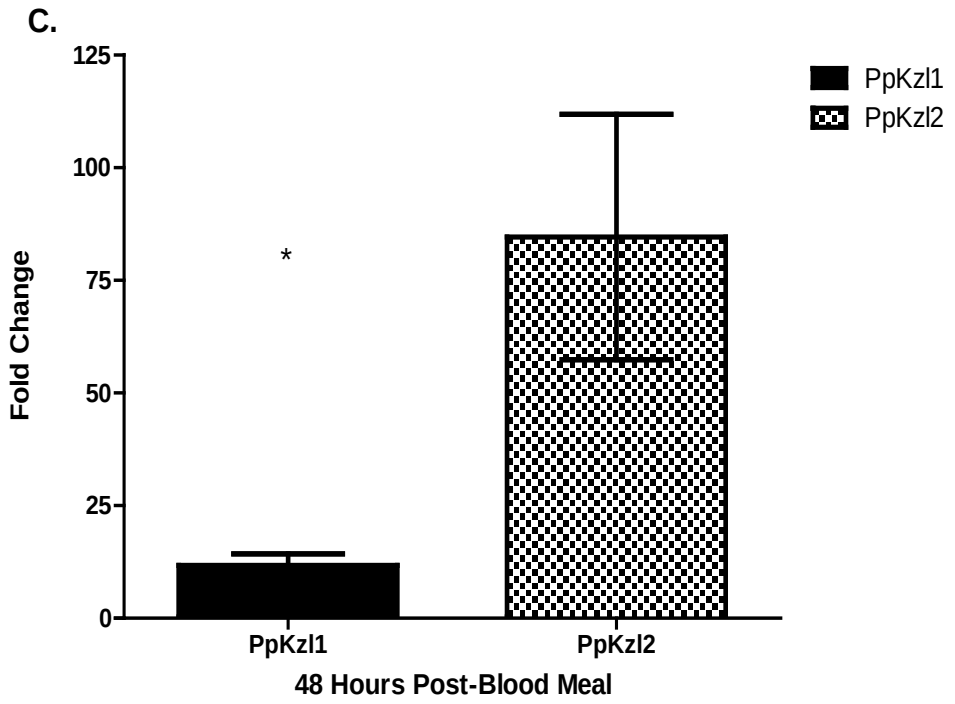

Figure 4 *PpKzl1* and *PpKzl2* expression in adult females post-blood meal. *PpKzl1* and *PpKzl2* mRNA expression levels are regulated after a blood meal. (A) *PpKzl1* is up-regulated 24 and 48 h post-blood meal with highest expression at 48 h post-blood meal. By 72 h expression is down-regulated to levels similar to 0 h. (B) *PpKzl2* is up-regulated 24, 48 and 72 h post-blood meal. Expression is highest at 48 h and decreases between 48-72 h post-blood meal. (C) *PpKzl1* and *PpKzl2* fold change at each time point is similar and differs only at 48 h post-blood meal when *PpKzl2* up-regulation is significantly higher than *PpKzl1* up-regulation. Values are means of individual midguts with standard error. Expression was normalized to *40S ribosomal protein S3* expression and calibrated to 0 h expression levels. Analysis used ANOVA t test with the Bonferroni correction for multi-comparisons (* = $p < 0.05$, ** = $p < 0.01$, *** = $p < 0.001$)

Primer Name	Primer Sequence 5'-3' Forward	Primer Sequence 5'-3' Reverse	Annealing ^{0}C	PCR
PpKzl859	GCACCAGCCCAAAAGACC	TCACTGCAATCTGATGGCGC	56.5	PCR
VR1020	ACAGGAGTCCAGGGCTGGAGAGAA	AGTGGCACCTTCCAGGGTCAAGGA	49	PCR
PpKzl1_137	AGAGCGTTACCTGTCCTTG	CCAGCGAATACTGAGGTTC	58	rt-PCR
PpKzl2_152	AATGAATGTCTGAAGGCCTG	CCTTGGGATTTCACCTCCC	58	rt-PCR
Pp40S_S3_136	GGACAGAAATCATCATCATG	CCTTTTCAGCGTACAGCTC	58	rt-PCR
PpKzl1_T7i	*T7*-GAAGAGCGCGTTACCTGTCC	*T7*-TTACCACAAATCACCATCAC	55	PCR (td)
PpKzl2_T7i	*T7*-GCACCAGCCCAAAAGACC	*T7*-TCACTGCAATCTGATGGCGC	58	PCR (td)
T7	TAATACGACTCACTATAGGG	TAATACGACTCACTATAGGG	58	PCR (td)
PpKzl2-R-His	His tag-CTGCAATCTGATGGCGC	TCACTGCAATCTGATGGCGC	60	PCR (td)

T7 promotor (*T7*)- TAATACGACTCACTATAGGGAGA (td) =Touchdown
His tag-TCAGTGGTGATGGTGATGATG

Table 1 Complete list of primers. Oligonucleotide primers for PCR reactions were designed specific to each cDNA sequence. Primer name, forward primer sequence, reverse primer sequence, annealing temperature (^{o}C**),** and PCR reaction type is listed for each primer set.

dsRNA injection

Effects of dsRNA injection on mRNA levels were assessed with rt-PCR and the comparative C_T method. Sand flies were injected with 90 ng of dsPpKzl1 or dsGFP. Relative expression levels of *PpKzl1* mRNA were compared between dsPpKzl1 injected and dsGFP injected sand flies at 4, 8, 12, 24, 30, 48, and 72 h post-injection (three independent experiments) (Figure 5 A). Relative expression levels were also measured post-blood meal at 24, 48, 72, and 96 h (two independent experiments combined) (Figure 5B). *PpKzl1* mRNA expression was not significantly reduced in the midgut at observed time points before and after a blood meal.

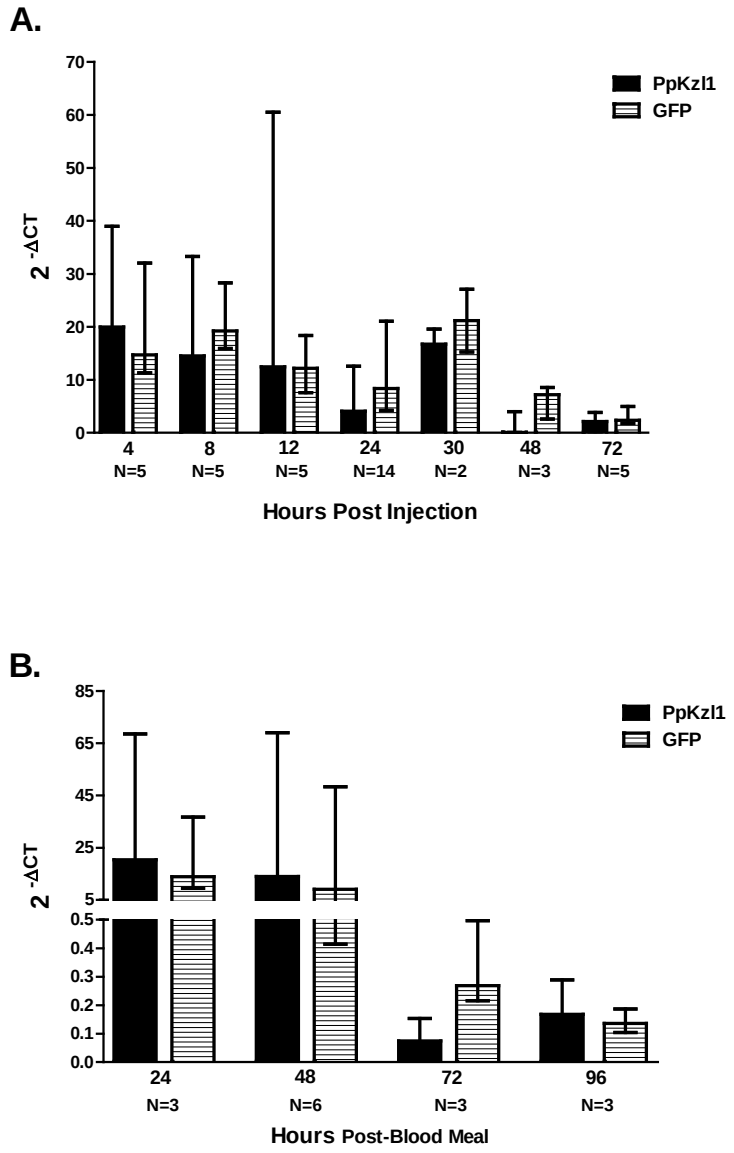

Figure 5 dsRNA effects on *PpKzl1* expression. PPIS flies were injected with dsPpKzl1 or control dsGFP. Relative expression levels of mRNA transcripts were assessed using rt-PCR. (A) *PpKzl1* expression 4, 8, 12, 24, 30, 48, and 72 h post-injection. (B) A blood meal was given 48 h post-injection and expression was measured at 24, 48, 72, and 96 h post-blood meal. C_T values were normalized to the expression of *40S ribosomal protein S3* gene and transformed to $2^{-\Delta CT}$. Each bar represents the median and interquartile range of expression in individual sand flies at each time point (N= number of individual sand flies used). Statistical analysis using a two-tailed Mann-Whitney U test found no statistical differences in relative expression between dsPpKzl1 and dsGFP injected sand flies.

For *PpKzl2* RNAi studies, sand flies were injected with 127 ng of dsPpKzl2 or dsGFP and relative expression levels of *PpKzl2* mRNA were measured at 6, 18, 24, 30, and 48 h post-injection (Figure 6A). For blood-induced expression analysis, sand flies were dissected 24 and 48 h post-blood meal (two independent experiments) (Figure 6B). *PpKzl1* mRNA expression was compared to control dsGFP injected sand flies at each time point. There was no significant reduction in *PpKzl2* mRNA relative expression levels observed in the midgut before or after a blood meal. Data was tested for normality with the Kolmogorov-Smirnov test and a two-tailed Mann-Whitney U test was used for nonparametric statistical analysis.

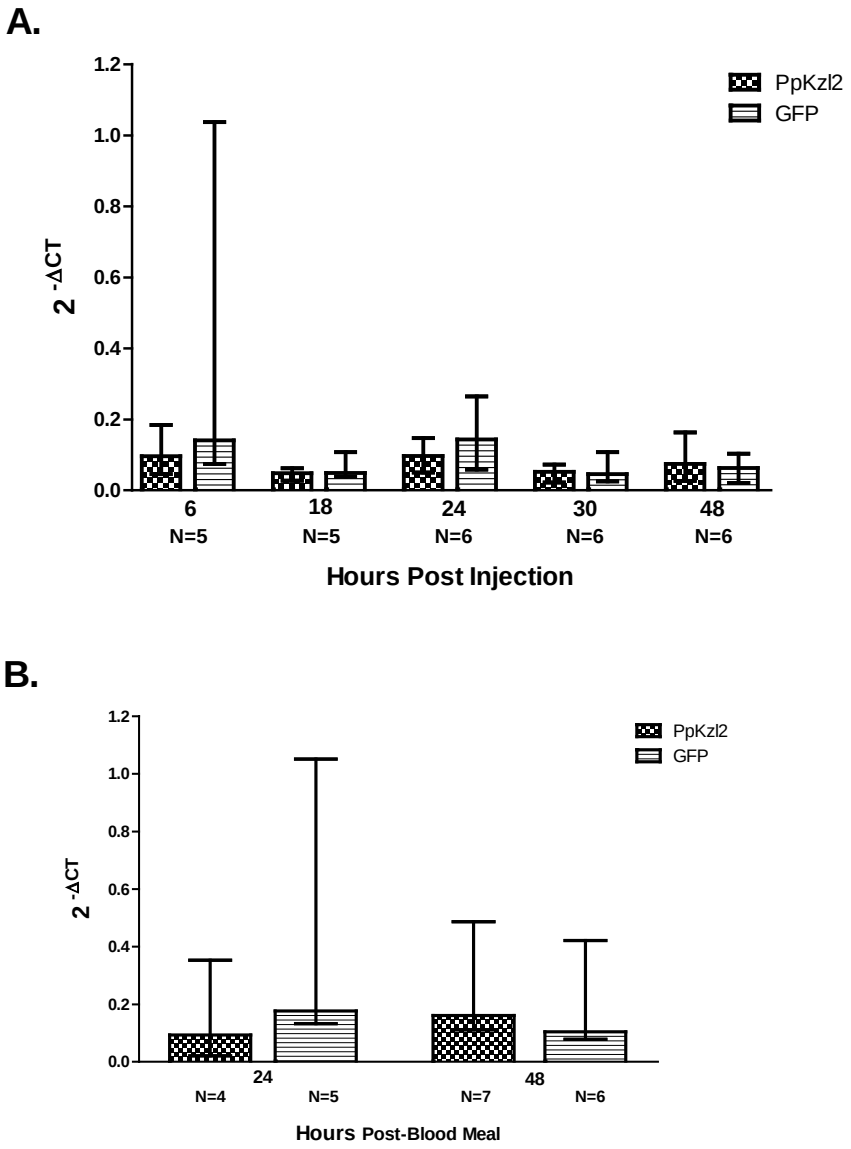

Figure 6 dsRNA effects on *PpKzl2* expression. Sand flies were injected with dsPpKzl2 or control dsGFP. Relative expression levels of mRNA transcripts were assessed using rt-PCR. (A) PPJO *PpKzl2* expression 6, 18, 24, 30, and 48 h post-injection. (B) PPIS *PpKzl2* expression post-blood meal. A blood meal was given 48 h post-injection and expression was analyzed at 24 and 48 h post- blood meal. C_T values were normalized to the expression of *40S ribosomal protein S3* and transformed to $2^{-\Delta CT}$. Each bar represents the median and interquartile range of expression in individual sand flies at each time point (N= number of individual sand flies used). Statistical analysis using a two-tailed Mann-Whitney U test found no statistical differences in relative expression between dsPpKzl2 and dsGFP injected sand flies.

Concurrently, to determine if injection of dsPpKzl2 affects blood meal digestion, hemoglobin was measured in blood meal remnants from dissected midguts of fully fed sand flies. Hemoglobin in dsPpKzl2 and dsGFP injected PPIS was measured at different stages of digestion at 24 and 48 h post-blood meal. The mean average hemoglobin in individual midguts of dsPpKzl2 injected flies was not significantly different from the mean average of dsGFP injected flies. There was no indication of dsPpKzl2 having an affect on the amount of hemoglobin in the midgut during blood meal digestion (Figure 7). This was consistent with *Ppkzl2* mRNA expression in Figure 6B. Data was tested for normality with the Kolmogorov-Smirnov test and a two-tailed unpaired t test was used for parametric statistical analysis.

For additional assessment of phenotypes, pictures were taken of midguts dissected for 48 h post-blood meal hemoglobin analysis. Variation in the amount of blood meal remnants in the midgut throughout both sample groups (Figure 8 and Figure 9) was consistent with the variation of hemoglobin observed in Figure 7. A range of stages from intermediate to complete digestion were observed in both dsPpKzl2 and dsGFP injected samples (empty midguts not pictured). Samples from both groups also had blood meal remnants in the hindgut as pictured in Figure 8A and Figure 8D.

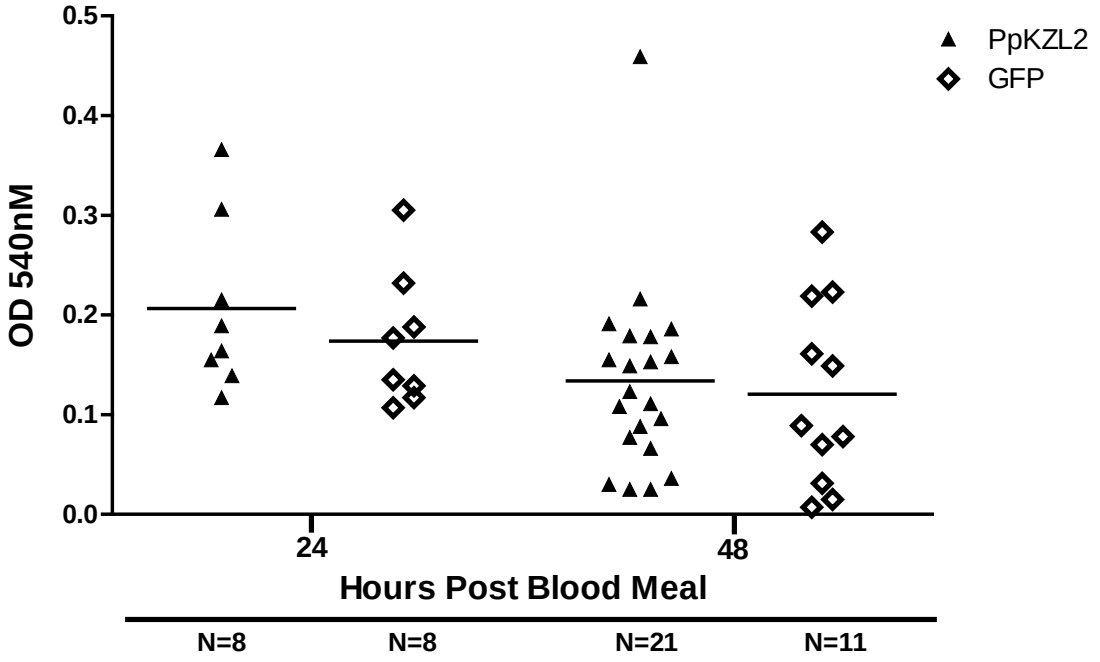

Figure 7 dsPpKzl2 effect on hemoglobin levels during blood meal digestion. PPIS were injected with dsPpKzl2 or control dsGFP and a blood meal was given 48 h post-injection. Sand fly midguts were dissected 24 and 48 h post-blood meal. Total hemoglobin in dissected midguts was quantified with a colorimetric assay using Drabkin's solution. There were no statistical differences in the means of dsPpKzl2 and dsGFP injected sand flies at 24 and 48 h post-blood meal. Absorbance was measured at 540 nm. Bars represent the mean of individual midguts (N= number of individual sand flies used). A two-tailed unpaired t test was used for statistical analysis.

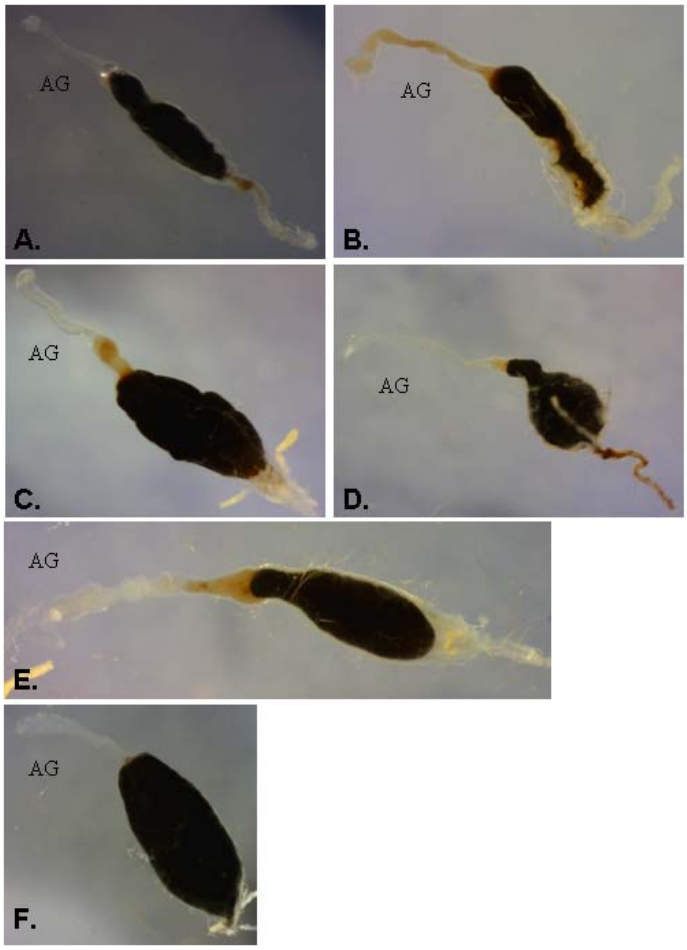

Figure 8 dsPpKzl2 injected midguts 48 post-blood meal. Midguts were dissected 48 h post-blood meal from sand flies injected with dsPpKzl2. (A-F) Pictures were taken on a dissecting microscope with an AM423X Dino-Eye camera and then midguts were used for hemoglobin analysis. Blood meal remnants were also seen in the hindgut in some samples (A and D). AG= anterior gut.

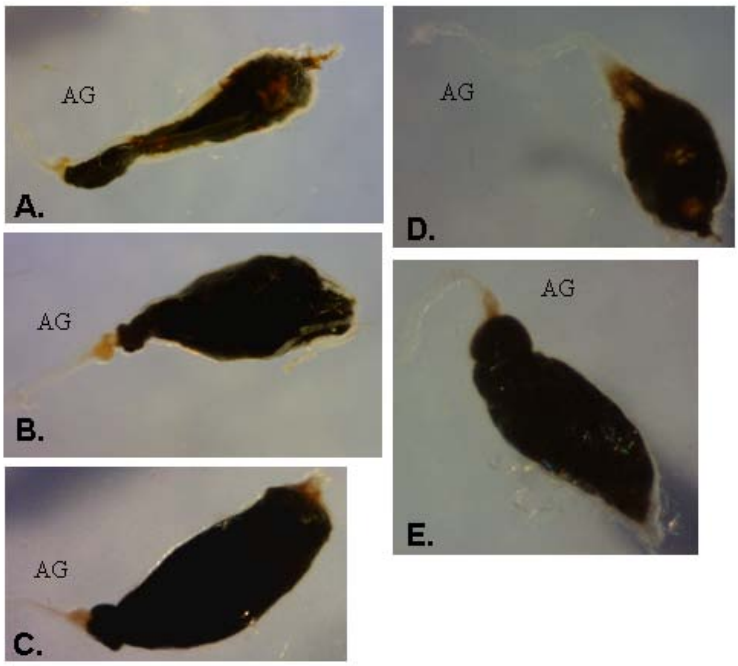

Figure 9 dsGFP injected midguts 48 h post-blood meal. Midguts were dissected 48 h post-blood meal from sand flies injected with dsGFP. (A-E) Pictures were taken on a dissecting microscope with an AM423X Dino-Eye camera and then midguts were used for hemoglobin analysis. AG= anterior gut.

Inhibition Assays

Inhibition activity of rPpKzl2 was tested for thrombin, trypsin, and α-chymotrypsin enzymes. Enzyme concentrations were kept constant and activity was tested with varying concentrations of substrate and rPpKzl2. The Michaelis-Menten equation was used to calculate V_{max} and K_m. Increasing concentrations of rPpKzl2 decreased V_{max} and K_m values for all three serine proteinases. Inhibition activity was measured as residual activity of the V_{max}. Inhibition activity of rPpKzl2 decreased both the V_{max} and K_m, which is representative of uncompetitive inhibition. Uncompetitive inhibition occurs when an inhibitor has high affinity to the enzyme-substrate complex and has little affinity or does not bind at all to the free enzyme (Copeland 2005). Dissociation constant αK_i was calculated for uncompetitive inhibition.

rPpKzl2 inhibited α-chymotrypsin activity and also weakly inhibited trypsin and thrombin activities. Inhibition of α-chymotrypsin occurred with an αK_i of 0.027 nM and residual activity of 9.4% of uninhibited α-chymotrypsin activity. Inhibition of thrombin by rPpKzl2 had an αK_i of 4.864 μM with 33% residual activity. Trypsin inhibition had an αK_i of 0.5931 μM and residual activity of 68%. rPpKzl2 had a higher affinity for trypsin than thrombin, however trypsin activity was the least inhibited. The highest affinity and reduction in serine proteinase activity by rPpKzl2 was exhibited for α-chymotrypsin.

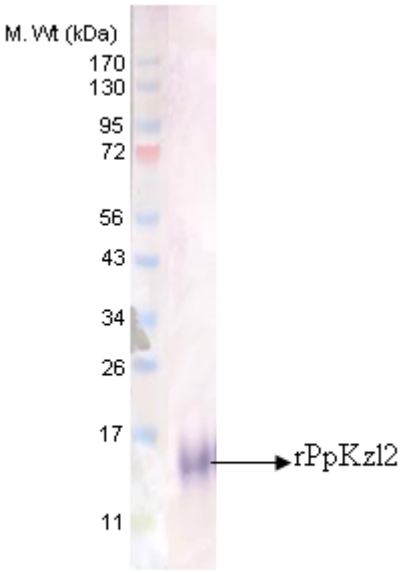

Figure 10 Purified rPpKzl2. Western blot of purified rPpKzl2 (6x His-tagged) using anti-His antibody. The recombinant protein showed a higher molecular weight than predicted by bioinformatics tools (7.6 kDa**)**. This is likely due to post translational modifications (e.g., glycosylation) generated by the CHO-S cells.

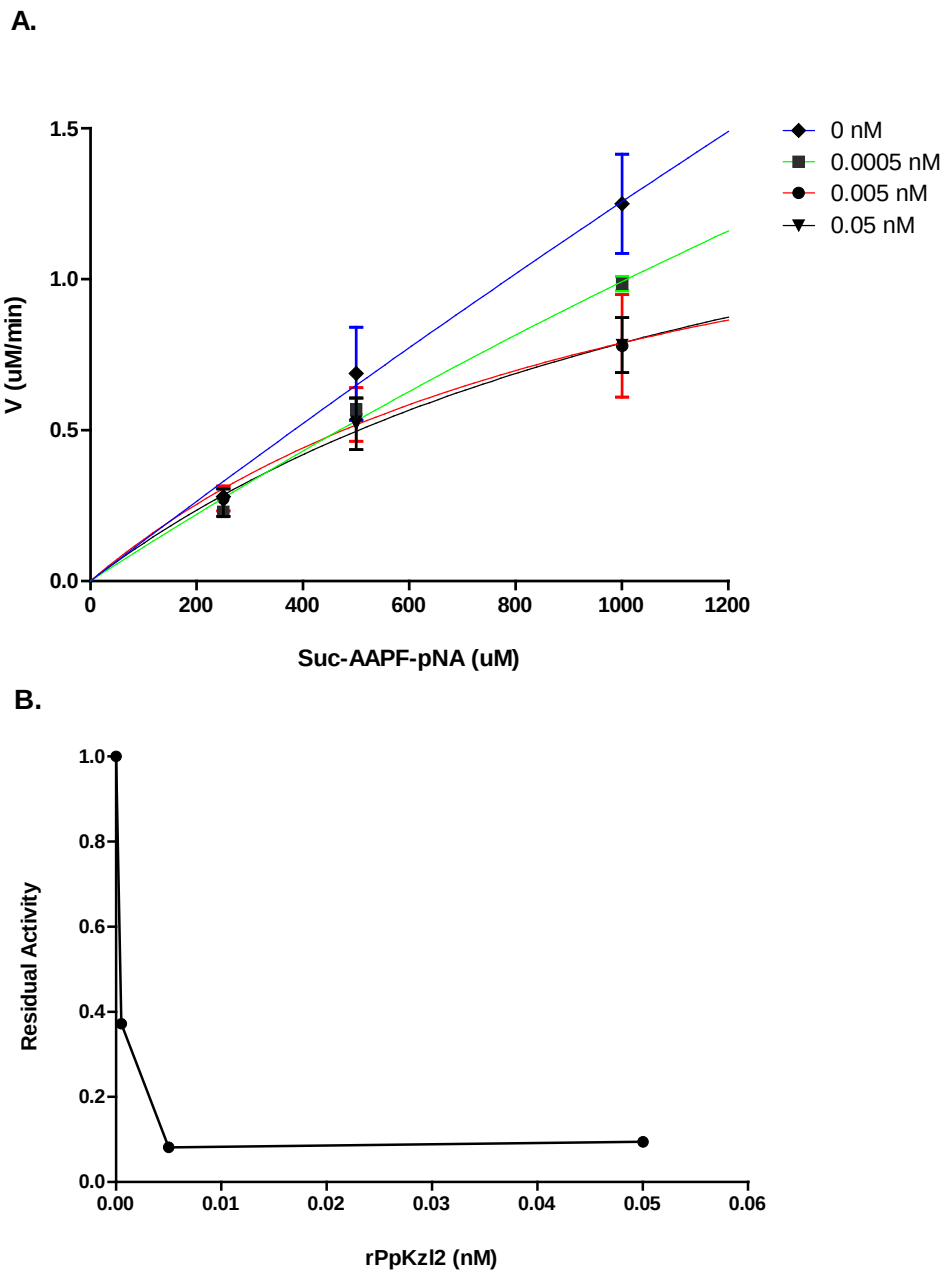

Figure 11 rPpKzl2 α-chymotrypsin activity. Reactions of 0.25 µM α-chymotrypsin with rPpKzl2 0.05, 0.005 or 0.0005 nM were initiated with addition of 250, 500, and 1000µM Suc-AAPF-pNA in 50 mM Tris-HCl pH 8.0. (A) Initial velocity over substrate concentration was fit with Michaelis-Menten non-linear regression for each concentration of rPpKzl2. A reduction in V_{max} and K_m values was observed with increasing rPpKzl2. Dissociation constant αKi = 0.027 nM. (B) Residual activity of α-chymotrypsin with increasing concentrations of rPpKzl2. Activity of α-chymotrypsin was reduced to 9.4% at 0.05 nM rPpKzl2.

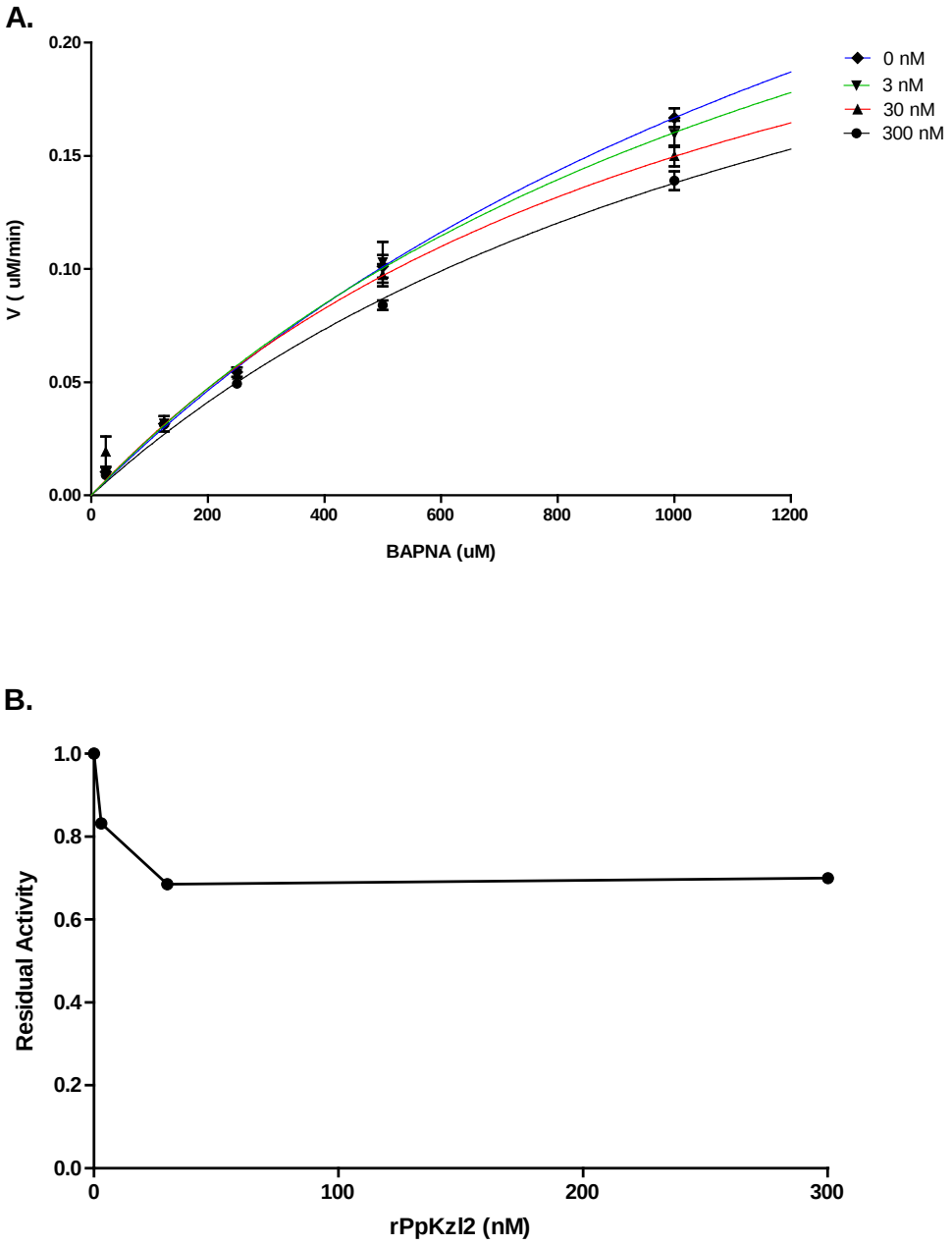

Figure 12 rPpKzl2 trypsin activity. Trypsin activity (2 µM) was measured at 3, 30, and 300 nM rPpKzl2 with 25, 125, 250, 500, and 1000 µM BAPNA. (A) Initial velocity over substrate concentration was fit with Michaelis-Menten non-linear regression for each concentration of rPpKzl2. Kinetic constants V_{max} and K_m decrease with increasing rPpKzl2. Dissociation constant αKi = 0.593 µM. (B) Residual activity of trypsin in the presence of increasing concentrations of rPpKzl2. Activity of trypsin was reduced to 68% at 30 and 300 nM rPpKzl2.

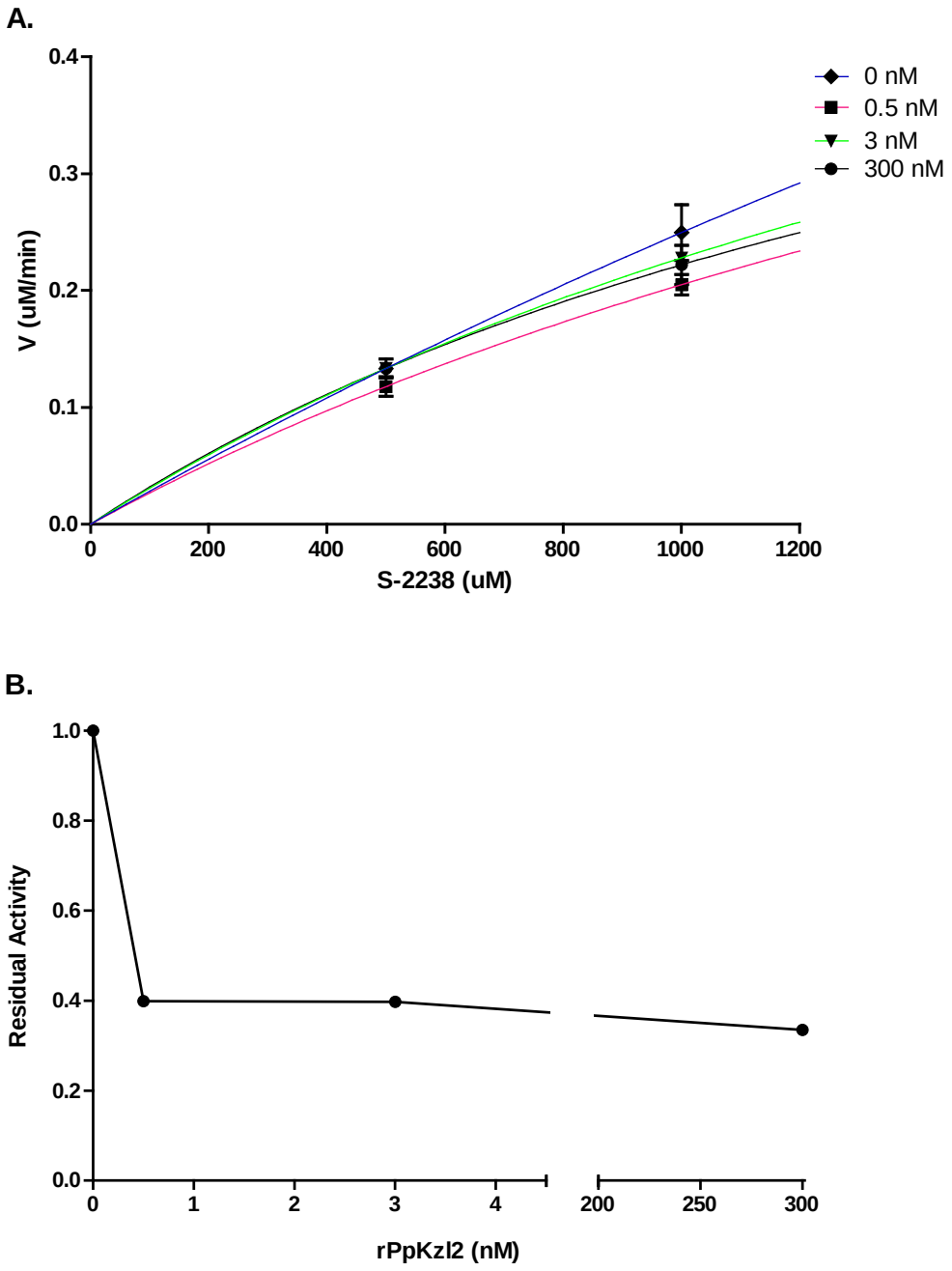

Figure 13 rPpKzl2 thrombin activity. The activity of 0.05 µM thrombin was measured at increasing concentrations 0.5, 3, and 300 nM rPpKzl2 with 500 and 1000 µM S-2238. (A) Initial velocity over substrate concentration was fit with Michaelis-Menten non-linear regression for each concentration of rPpKzl2. Inhibition of thrombin was observed with decreasing V_{max} and K_m values with a dissociation constant αKi = 4.864 µM. (B) Residual activity of thrombin in the presence of rPpKzl2. Thrombin activity was reduced to 33% residual activity.

Serine Proteinase	rPpKzl2 (nM)	Inhibiton (%)	Vmax (uM/min)	Km (uM)	r^2	αK_i
Thrombin	0	-	1.979	6929	0.74	4.864 μM
	0.5	60.1	0.789	2850	0.87	-
	3	60.3	0.786	2448	0.96	-
	300	66.5	0.663	1985	0.87	-
Trypsin	0	-	0.523	2276	0.99	0.593 μM
	3	27.3	0.380	1607	0.99	-
	30	40.1	0.313	1237	0.95	-
	300	36.0	0.334	1424	0.99	-
Chymotrypsin	0	-	20.32	15163	0.82	0.027 nM
	0.0005	62.8	7.557	6614	0.97	-
	0.005	91.8	1.664	1108	0.61	-
	0.05	90.5	1.921	1436	0.79	-

Table 2 Inhibition activity of different serine proteinases by rPpKzl2. rPpKzl2 values of percent inhibition, V_{max}, K_m, r^2 and αK_i for thrombin, trypsin, and α-chymotrypsin inhibition. The V_{max} and K_m values were calculated with the Michaelis-Menten equation with dissociation constant αKi for uncompetitive inhibition.

Discussion

In *P. papatasi*, two putative Kazal-type inhibitors, *PpKzl1* and *PpKzl2,* were identified following analyses of the midgut transcriptome. Kazal-type inhibitors have been indentified in blood feeding arthropods as inhibitors of thrombin and coagulation cascade factors.

The predicted amino acid sequences of PpKzl1 and PpKzl2 display some similarities but also have differences in residues important for structure and function. Cysteine location differences between PpKzl1 and PpKzl2 may cause differences in disulfide bridge formation (Rimphanitchayakit and Tassanakajon 2010). However, the number of amino acid residues between cysteines 2 and 3, containing the predicted P1 residue, is the same for PpKzl1 and PpKzl2. The PpKzl1 predicted P1 site has an arginine, a basic residue, and PpKzl2 has a tyrosine, an aromatic hydrophobic residue. These differences in structure and active site residues propose different functions for PpKzl1 and PpKzl2. Basic amino acids in the P1 site are predicted to inhibit trypsin and thrombin, and bulky hydrophobic amino acids are predicted to inhibit chymotrypsin (Donpudsa et al. 2009). Both PpKzl1 and PpKzl2 are similar to putative proteins in *L. longipalpis.* While the PpKzl1 predicted P1 residue is conserved between *P. papatasi* and *L. longipalpis* the *L. longipalpis* Kzl2 has a phenylalanine in the P1 site where PpKzl2 has a tyrosine.

Interestingly, earlier studies of blood feeding insects from which Kazal thrombin-specific inhibitors were characterized, have identified only a single Kazal-type inhibitor (Tanaka-Azevedo et al. 2010). In *P. papatasi* two Kazal-type inhibitors were identified in the midgut. This seems to be prevalent in other dipteran species as we found multiple species with transcripts similar to both *PpKzl1* and *PpKzl2*. This includes *L. longipalpis, An. darlingi, Ae. aegypti, An. gambiae, D. pseudobscura,* and *Cx. Quinquefasciatus* and some species having even more than two transcripts containing Kazal-type domains.

PpKzl1 is similar to inhibitors of trypsin, thrombin, Factor XIIa, plasmin, and subtilisin found in various tissues including midguts, salivary glands, ovaries and fat bodies. While the activity of these inhibitors has been described, *in vitro* functional characterization of target proteinases is yet to be determined. *PpKzl2* is similar to proteins with Kazal-type domains found in hemocytes, larval fat body, bristles and midgut. Of these sequences several are putative

proteins identified in cDNA libraries of immune challenged individuals, and activity of these proteins is unknown. Cocoons of the greater wax moth, *Galleria mellonella*, contain a Kazal-type inhibitor that was identified in silk extracted from cocoons. With a threonine in the P1 site, this Kazal inhibits proteinase K and subtilisin, weakly inhibits trypsin, and no activity was observed for chymotrypsin (Nirmala et al. 2001). This is the only Kazal inhibitor with demonstrated activity that is similar to PpKzl2, with sequence identity of 27% and 45% similarity.

Temporal analysis of *PpKzl1* and *PpKzl2* mRNA transcripts indicate similarities in expression profiles. *PpKzl1* and *PpKzl2* mRNA transcripts are found to be expressed in non blood-fed and blood-fed females, with the expression in blood-fed females regulated by the blood meal. Both *PpKzl1* and *PpKzl2* mRNA transcripts are up-regulated at 24 and 48 h post-blood meal, suggesting that the protein may have a functional role in blood meal digestion. PpKzl1 is predicted to inhibit trypsin and rPpKzl2 inhibits chymotrypsin with a high affinity. Trypsin and chymotrypsin activity in the *P. papatasi* midgut are temporally similar (Ramalho-Ortigão et al. 2003). Two chymotrypsin-like and four trypsin-like proteins have been identified in *P. papatasi* midgut cDNA libraries. Low levels of trypsin activity was first detected at 1 h post-blood meal and decreased to baseline levels by 72 h, and chymotrypsin activity was first detected at 6 h and by 72 h was no longer detected (Ramalho-Ortigão et al. 2003). This correlates with levels of *PpKzl1* and *PpKzl2* mRNA expression occurring between 24-48 h post-blood meal when both trypsin and chymotrypsin enzyme activity is observed. Interestingly, the decrease in *PpKzl1* and *PpKzl2* expression detected around 72 h post-blood meal also correlates with the completion of blood meal digestion, which culminates with the midgut emptying between 72-144 h post-blood meal.

PpKzl1 is predicted to inhibit trypsin-like serine proteinases, particularly thrombin and trypsin. The amino acid sequence of PpKzl1 showed highest similarities to Kazal domains with trypsin and thrombin activity. Kazal inhibitors have shown activity for proteinases different from predicted activity of the P1 residue (Augustin et al. 2009). While inferences from sequence similarities are insightful, the variation in activity among Kazal inhibitors is large and activity should be deduced from biochemically characterization.

The rPpKzl2 inhibits α-chymotrypsin and also has some activity for thrombin and trypsin. Activity of the rPpKzl2 arginine P1 residue was predicted to inhibit α-chymotrypsin.

Inhibitory activity of rPpKzl2 is uncompetitive in nature, decreasing both K_m and V_{max} values with increasing concentrations of rPpKzl2. rPpKzl2 is an uncompetitive inhibitor and therefore has higher affinity to the enzyme-substrate complex and little to no affinity for the free enzyme (Copeland 2005). Surprisingly rPpKzl2 also weakly inhibited thrombin and trypsin. Other single-domain Kazal-type inhibitors have activity for multiple serine proteinases (Nirmala et al. 2001; Watanabe et al. 2010). The ability of PpKzl2 to inhibit serine proteinases in *P. papatasi* midgut is dependent upon the rate of inhibition and concentrations present in the midgut (Kanost and Jiang 1996). *In vitro* assays may not be complete indications of *in vivo* activity.

PpKzl1 is predicted to have activity for trypsin because of its P1 residue. It has been suggested that overlapping activity may exist, to prevent unregulated proteinase cascades from causing harm in case of function issues or depletion of the regulating inhibitor (Kanost and Jiang 1996). This may be the case for PpKzl1 and PpKzl2. Suggestions of inhibitors with dual inhibition of both native and exogenous proteinases have also been made (Shenoy et al. 2011). PpKzl1and PpKzl2 may differ in specificity for different trypsin proteinases.

We did not observe a knockdown affect in mRNA expression levels using RNAi by microinjection for *PpKzl2* and *PpKzl1* in the midgut of *P. papatasi*. Previous work in *P. papatasi* has shown that dsRNA injections within this range of concentrations resulted in a reduction in expression of midgut transcripts (Coutinho-Abreu et al. 2011) and also in *L. longipalpis* (Sant'Anna et al. 2009; Sant'Anna et al. 2008). While there was no significant difference, percent mRNA expression in dsPpKzl2 injected flies was consistently lower than with dsGFP injected flies up to 30 h post-injection. It is possible that silencing of these genes may require highly concentrated amounts of dsRNA. Concurrently, the amount of hemoglobin in the midgut of injected flies was measured and also was not significantly different for dsPpKzl2 and dsGFP.

It has been described that in sand flies infection with *Leishmania* leads to modulation of trypsin-like activity in the midgut during digestion, suggesting that modulation of trypsin activity allows the parasites to survive (Borovsky and Schlein 1987; Sant'Anna et al. 2009; Telleria et al. 2010). This has been supported with data showing that RNAi of a trypsin gene increased parasite numbers during infection (Sant'Anna et al. 2009). rPpKzl2 inhibited chymotrypsin and weakly inhibited trypsin. The dynamics of serine proteinases and serine proteinase inhibitors in the midgut are not only crucial to sand fly metabolism and digestion, but may also affect *Leishmania* development (Jiang and Kanost 2000).

While PpKzl1 is predicted to have thrombin inhibitory activity, we observed thrombin inhibition by rPpKzl2. Thrombin inhibition in blood feeding arthropods prevents coagulation of ingested blood meals. In addition to regulation of digestive proteinases, PpKzl2 may also regulate blood fluidity within the midgut. Further characterization of the serine proteinase cascades and their inhibitors in *P. papatasi* may provide insight into the complex interactions that constitute vector competence.

Conclusions

The objectives of this project were to characterize *PpKzl1* and *PpKzl2* with molecular and biochemical techniques. Our data show that *PpKzl1* and *PpKzl2* are both constitutively expressed in the midgut and tightly regulated by a blood meal. We were not able to functionally analyze *PpKzl1* and *PpKzl2* using RNAi. Different applications of RNAi or different approaches are suggested for future work.

The rPpKzl2 displayed activity for chymotrypsin, trypsin and thrombin suggesting that PpKzl2 is an active Kazal-type inhibitor within the midgut. As single Kazal-type domains can inhibit multiple proteinases it would be useful to test rPpKzl2 also for activity of subtilisin, elastase, and proteinase K and further characterization of rPpKzl2 thrombin inhibition could be assessed with activity assays for thrombin induced platelet aggregation, thrombin clotting time, and activated partial thromboplastin time. We are also interested in further characterizing the interactions between rPpKzl2 and serine proteinases. Future plans also include the biochemical characterization of a recombinant PpKzl1 using inhibition assays similar to the ones used in this study.

Ultimately, characterization of protein activity in the midgut and identification of target proteinases in *P. papatasi* are required for evaluating the roles PpKzl1 and PpKzl2 play in regulating serine proteinase cascades as well as possible effects on *Leishmania* development.

We are further interested in *PpKzl1* and *PpKzl2* as possible candidates for TBV's, as we have described both transcripts as tightly regulated by a blood meal and PpKzl2 as a possible inhibitor of digestive proteinases and thrombin in the midgut.

References

Altschul S. F., Madden T. L., Schäffer A. A., Zhang J., Zhang Z., Miller W. and Lipman D. J. 1997. Gapped BLAST and PSI-BLAST: a new generation of protein database search programs. Nucleic acids research 25: 3389-3402.

Arakane Y., Li B., Muthukrishnan S., Beeman R. W., Kramer K. J. and Yoonseong P. 2008. Functional analysis of four neuropeptides, EH, ETH, CCAP and bursicon, and their receptors in adult ecdysis behavior of the red flour beetle, *Tribolium castaneum*. Mechanisms of development 125: 984.

Araujo R. N., Campos I. T. N., Tanaka A. S., Santos A., Gontijo N. F., Lehane M. J. and Pereira M. H. 2007. Brasiliensin: A novel intestinal thrombin inhibitor from *Triatoma brasiliensis* (Hemiptera: Reduviidae) with an important role in blood intake. International journal for parasitology 37: 1351.

Augustin R., Siebert S. and Bosch T. C. G. 2009. Identification of a kazal-type serine protease inhibitor with potent anti-staphylococcal activity as part of Hydra's innate immune system. Developmental & Comparative Immunology 33: 830-837.

Bartholomay L. C., Cho W., Rocheleau T. A., Boyle J. P., Beck E. T., Fuchs J. F., Liss P., Rusch M., Butler K. M., Wu R. C., Lin S., Kuo H., Tsao I., Huang C., Liu T., Hsiao K., Tsai S., Yang U., Nappi A. J., Perna N. T., Chen C. and Christensen B. M. 2004. Description of the Transcriptomes of Immune Response-Activated Hemocytes from the Mosquito Vectors *Aedes aegypti* and *Armigeres subalbatus*. Infection and immunity 72: 4114-4126.

Bates P. A. 2008. *Leishmania* sand fly interaction: progress and challenges. Current opinion in microbiology 11: 340.

Bates P. A. 2007. Transmission of *Leishmania* metacyclic promastigotes by phlebotomine sand flies. International journal for parasitology 37: 1097-1106.

Borovsky D. and Schlein Y. 1987. Trypsin and chymotrypsin-like enzymes of the sandfly *Phlebotomus papatasi* infected with Leishmania and their possible role in vector competence. Medical and veterinary entomology 1: 235-242.

Calvo E., Pham V., Marinotti O., Andersen J. and Ribeiro J. 2009. The salivary gland transcriptome of the neotropical malaria vector *Anopheles darlingi* reveals accelerated evolution of genes relevant to hematophagy. BMC Genomics 10: 57.

Campbell C. L., Vandyke K. A., Letchworth G. J., Drolet B. S., Hanekamp T. and Wilson W. C. 2005. Midgut and salivary gland transcriptomes of the arbovirus vector *Culicoides sonorensis* (Diptera: Ceratopogonidae). Insect molecular biology 14: 121-136.

Campos I. T., Amino R., Sampaio C. A., Auerswald E. A., Friedrich T., Lemaire H. G., Schenkman S. and Tanaka A. S. 2002. Infestin, a thrombin inhibitor presents in *Triatoma infestans* midgut, a Chagas' disease vector: gene cloning, expression and characterization of the inhibitor. Insect biochemistry and molecular biology 32: 991-997.

Campos I. T., Tanaka-Azevedo A. M. and Tanaka A. S. 2004. Identification and characterization of a novel factor XIIa inhibitor in the hematophagous insect, *Triatoma infestans* (Hemiptera: Reduviidae). FEBS letters 577: 512-516.

Cappello M., Li S., Chen X., Li C. B., Harrison L., Narashimhan S., Beard C. B. and Aksoy S. 1998. Tsetse thrombin inhibitor: bloodmeal-induced expression of an anticoagulant in salivary glands and gut tissue of *Glossina morsitans morsitans*. Proceedings of the National Academy of Sciences of the United States of America 95: 14290-14295.

Coutinho-Abreu I. V. and Ramalho-Ortigão M. 2010. Transmission blocking vaccines to control insect-borne diseases: a review. Memórias do Instituto Oswaldo Cruz 105: 1.

Copeland R. A. 2005. Evaluation of Enzyme Inhibitors in Drug Discovery : A Guide for Medicinal Chemists and Pharmacologists. John Wiley & Sons, Inc. (US), Hoboken, N.J.

Copeland R. A. 2000. Enzymes: a practical introduction to structure, mechanism, and data analysis, 2nd ed. John Wiley & Sons, Inc. (US), Hoboken, N.J.

Coutinho-Abreu I. V., Sharma N. K., Robles-Murguia M. and Ramalho-Ortigao M. Targeting the Midgut Secreted PpChit1 Reduces *Leishmania major* Development in Its Natural Vector, the Sand Fly *Phlebotomus papatasi*. PLoS Negl Trop Dis : e901.

Di Cera E. 2009. Serine proteases. IUBMB life 61: 510-515.

Donpudsa S., Tassanakajon A. and Rimphanitchayakit V. 2009. Domain inhibitory and bacteriostatic activities of the five-domain Kazal-type serine proteinase inhibitor from black tiger shrimp *Penaeus monodon*. Developmental & Comparative Immunology 33: 481-488.

Francischetti I. M. B., Valenzuela J. G. and Ribeiro J. M. C. 1999. Anophelin: Kinetics and Mechanism of Thrombin Inhibition Biochemistry 38: 16678-16685.

Friedrich T., Kröger B., Bialojan S., Lemaire H. G., Höffken H. W., Reuschenbach P., Otte M. and Dodt J. 1993. A Kazal-type inhibitor with thrombin specificity from *Rhodnius prolixus*. Journal of Biological Chemistry 268: 16216.

Gandhe A., Arunkumar K., John S. and Nagaraju J. 2006. Analysis of bacteria-challenged wild silkmoth, *Antheraea mylitta* (lepidoptera) transcriptome reveals potential immune genes. BMC Genomics 7: 184.

Gasteiger E., Gattiker A., Hoogland C., Ivanyi I., Appel R. D. and Bairoch A. 2003. ExPASy: the proteomics server for in-depth protein knowledge and analysis. Nucleic acids research 31: 3784-3788.

Hemmi H., Kumazaki T., Yoshizawa-Kumagaye K., Nishiuchi Y., Yoshida T., Ohkubo T. and Kobayashi Y. 2005. Structural and functional study of an Anemonia Elastase Inhibitor, a "Nonclassical" Kazal-type Inhibitor from *Anemonia sulcata*. Biochemistry 44: 9626.

Jiang H. and Kanost M. R. 2000. The clip-domain family of serine proteinases in arthropods. Insect Biochemistry and Molecular Biology 30: 95-105.

Kanost M. R. and Jiang H. 1996. Proteinase Inhibitors in Invertebrate Immunity. In: Söderhäll K., Iwanaga S., Vanta G., editors. New directions in invertebrate immunology. SOS Publications, Fair Haven, N.J., P. 155-174.

Kanost M. R. 1999. Serine proteinase inhibitors in arthropod immunity. Developmental & Comparative Immunology 23: 291-301.

Kimblin N., Peters N., Debrabant A., Secundino N., Egen J., Lawyer P., Fay M. P., Kamhawi S. and Sacks D. 2008. Quantification of the infectious dose of Leishmania major transmitted to the skin by single sand flies. Proceedings of the National Academy of Sciences 105: 10125-10130.

Larkin M. A., Blackshields G., Brown N. P., Chenna R., McGettigan P. A., McWilliam H., Valentin F., Wallace I. M., Wilm A., Lopez R., Thompson J. D., Gibson T. J. and Higgins D. G. 2007. Clustal W and Clustal X version 2.0. Bioinformatics 23: 2947-2948.

Livak K. J. and Schmittgen T. D. 2001. Analysis of Relative Gene Expression Data Using Real-Time Quantitative PCR and the $2^{-\Delta\Delta CT}$ Method. Methods 25: 402-408.

Meiser C. K., Piechura H., Werner T., Dittmeyer-Schäfer S., Meyer H. E., Warscheid B., Schaub G. A. and Balczun C. 2010. Kazal-type inhibitors in the stomach of Panstrongylus megistus (Triatominae, Reduviidae). Insect biochemistry and molecular biology .

Mende K., Lange U. and Nowak G. 2004. Three recombinant serine proteinase inhibitors expressed from the coding region of the thrombin inhibitor dipetalogastin. Insect biochemistry and molecular biology 34: 971-979.

Mende K., Petoukhova O., Koulitchkova V., Schaub G. A., Lange U., Kaufmann R. and Nowak G. 1999. Dipetalogastin, a potent thrombin inhibitor from the blood-sucking insect *Dipetalogaster maximus*. European Journal of Biochemistry 266: 583-590.

Nirmala X., Kodrik D., Zurovec M. and Sehnal F. 2001. Insect silk contains both a Kunitz-type and a unique Kazal-type proteinase inhibitor. European journal of biochemistry 268: 2064-2073.

Noeske-Jungblut C., Haendler B., Donner P., Alagon A., Possani L. and Schleuning W. 1995. Triabin, a Highly Potent Exosite Inhibitor of Thrombin. Journal of Biological Chemistry 270: 28629-28634.

Oliveira F., Kamhawi S., Seitz A. E., Pham V. M., Guigal P. M., Fischer L., Ward J. and Valenzuela J. G. 2006. From transcriptome to immunome: identification of DTH inducing proteins from a *Phlebotomus ariasi* salivary gland cDNA library. Vaccine 24: 374.

Paim R. M. M., Araújo R. N., Soares A. C., Lemos L. C. D., Tanaka A. S., Gontijo N. F., Lehane M. J. and Pereira M. H. 2011. Influence of the intestinal anticoagulant in the feeding performance of triatomine bugs (Hemiptera; Reduviidae). International journal for parasitology 41: 765-773.

Pitaluga A., Beteille V., Lobo A., Ortigão-Farias J., Dávila A., Souza A., Ramalho-Ortigão J. and Traub-Cseko Y. 2009. EST sequencing of blood-fed and *Leishmania*-infected midgut of *Lutzomyia longipalpis*, the principal visceral leishmaniasis vector in the Americas. Molecular Genetics and Genomics 282: 307-317.

Ramalho-Ortigão M., Jochim R., Anderson J., Lawyer P., Pham V., Kamhawi S. and Valenzuela J. 2007. Exploring the midgut transcriptome of *Phlebotomus papatasi*: comparative analysis of expression profiles of sugar-fed, blood-fed and *Leishmania major*-infected sandflies. BMC Genomics 8: 300.

Ramalho-Ortigão J. M., Kamhawi S., Rowton E. D., Ribeiro J. M. C. and Valenzuela J. G. 2003. Cloning and characterization of trypsin- and chymotrypsin-like proteases from the midgut of the sand fly vector *Phlebotomus papatasi*. Insect biochemistry and molecular biology 33: 163-171.

Ramalho-Ortigão M., Saraiva E. M. and Traub-Csekö Y. M. 2010. Sand Fly-Leishmania Interactions: Long Relationships are Not Necessarily Easy. The Open Parasitology Journal 4: 195.

Ricci C. G., Pinto A. F. M., Berger M. and Termignoni C. 2007. A thrombin inhibitor from the gut of Boophilus microplus ticks. Experimental Applied Acarology 42: 291-300.

Rimphanitchayakit V. and Tassanakajon A. 2010. Structure and function of invertebrate Kazal-type serine proteinase inhibitors. Developmental & Comparative Immunology 34: 377-386.

Sacks D. L. 2001. Leishmania-sand fly interactions controlling species-specific vector competence. Cellular microbiology 3: 189.

Sant'Anna M. R. V., Diaz-Albiter H., Mubaraki M., Dillon R. J. and Bates P. A. 2009. Inhibition of trypsin expression in Lutzomyia longipalpis using RNAi enhances the survival of Leishmania. Parasites & Vectors 2.

Sant'Anna M. R. V., Alexander B., Bates P. A. and Dillon R. J. 2008. Gene silencing in phlebotomine sand flies: Xanthine dehydrogenase knock down by dsRNA microinjections. Insect biochemistry and molecular biology 38: 652-660.

Saraiva E. M., Barbosa A. F., Santos F. N., Borja-Cabrera G. P., Nico D., Souza L. O. P., Mendes-Aguiar C. O., Souza E. P., Fampa P. and Parra L. E. 2006. The FML-vaccine (Leishmune®) against canine visceral leishmaniasis: a transmission blocking vaccine. Vaccine 24: 2423.

Schlott B., Wöhnert J., Icke C., Hartmann M., Ramachandran R., Gührs K., Glusa E., Flemming J., Görlach M., Große F. and Ohlenschläger O. 2002. Interaction of Kazal-type Inhibitor Domains with Serine Proteinases: Biochemical and Structural Studies. Journal of Molecular Biology 318: 533-546.

Schmittgen T. D. and Livak K. J. 2008. Analyzing real-time PCR data by the comparative CT method. Nature protocols 3: 1101.

Shenoy R. T., Thangamani S., Velazquez-Campoy A., Ho B., Ding J. L. and Sivaraman J. 2011. Structural Basis for Dual-Inhibition Mechanism of a Non-Classical Kazal-Type Serine Protease Inhibitor from Horseshoe Crab in Complex with Subtilisin. PLoS ONE 6: e18838.

Tanaka-Azevedo A. M., Morais-Zani K., Torquato R. J. S. and Tanaka A. S. 2010. Thrombin Inhibitors from Different Animals. Journal of Biomedicine and Biotechnology 2010.

Telleria E. L., Araújo A., Secundino N. F., d'Avila-Levy C. M. and Traub-Csekö Y. M. 2010. Trypsin-Like Serine Proteases in *Lutzomyia longipalpis* – Expression, Activity and Possible Modulation by *Leishmania infantum chagasi*. PLoS ONE : e10697.

van de Locht A., Lamba D., Bauer M., Huber R., Friedrich T., Kröger B., Höffken W. and Bode W. 1995. Two heads are better than one: crystal structure of the insect derived double domain Kazal inhibitor rhodniin in complex with thrombin. EMBO journal 14: 5149.

Veiga A. B. G., Ribeiro J. M. C., Guimarães J. A. and Francischetti I. M. B. 2005. A catalog for the transcripts from the venomous structures of the caterpillar *Lonomia obliqua*: Identification of the proteins potentially involved in the coagulation disorder and hemorrhagic syndrome. Gene 355: 11-27.

Watanabe R. M. O., Soares T. S., Morais-Zani K., Tanaka-Azevedo A. M., Maciel C., Capurro M. L., Torquato R. J. S. and Tanaka A. S. 2010. A novel trypsin Kazal-type inhibitor from *Aedes aegypti* with thrombin coagulant inhibitory activity. Biochimie 92: 933-939.

Waterhouse A. M., Procter J. B., Martin D. M. A., Clamp M. and Barton G. J. 2009. Jalview Version 2—a multiple sequence alignment editor and analysis workbench. Bioinformatics 25: 1189-1191.

WHO. 2010. Technical Report Series 949.Control of Leishmaniasis. Report of a meeting of the WHO Expert Committee on the Control of Leishmaniases.